Journal of Hydrology 502 (2013) 103–119

Contents lists available at ScienceDirect

Journal of Hydrology

journal homepage: www.elsevier.com/locate/jhydrol

Predictability of nonstationary time series using wavelet and EMD based ARMA models

L. Karthikeyan, D. Nagesh Kumar *

Department of Civil Engineering, Indian Institute of Science, Bangalore 560012, India

ARTICLE INFO

Article history:
Received 16 May 2013
Received in revised form 4 August 2013
Accepted 20 August 2013
Available online 27 August 2013
This manuscript was handled by Andras Bardossy, Editor-in-Chief, with the assistance of Attilio Castellarin, Associate Editor

Keywords:
Time series analysis
Prediction
Wavelets
Streamflow
Rainfall

SUMMARY

Research has been undertaken to ascertain the predictability of non-stationary time series using wavelet and Empirical Mode Decomposition (EMD) based time series models. Methods have been developed in the past to decompose a time series into components. Forecasting of these components combined with random component could yield predictions. Using this ideology, wavelet and EMD analyses have been incorporated separately which decomposes a time series into independent orthogonal components with both time and frequency localizations. The component series are fit with specific auto-regressive models to obtain forecasts which are later combined to obtain the actual predictions. Four non-stationary streamflow sites (USGS data resources) of monthly total volumes and two non-stationary gridded rainfall sites (IMD) of monthly total rainfall are considered for the study. The predictability is checked for six and twelve months ahead forecasts across both the methodologies. Based on performance measures, it is observed that wavelet based method has better prediction capabilities over EMD based method despite some of the limitations of time series methods and the manner in which decomposition takes place. Finally, the study concludes that the wavelet based time series algorithm can be used to model events such as droughts with reasonable accuracy. Also, some modifications that can be made in the model have been discussed that could extend the scope of applicability to other areas in the field of hydrology.

1. Introduction

Traditional time series forecasting is generally done using regression techniques. In the case of regression model, a relationship is built up between a set of explanatory variables and dependent variables. The coefficients or parameters in the relationship are obtained by various methods the earliest being Gauss's 'Least Squares (LS)' method in 1794. The LS method has poor extrapolation properties and is sensitive to outliers in the time series.

Moving average, weighted moving average, linear exponential smoothing, Kalman filters are some of the primitive forecasting techniques used by several groups (Macaulay, 1931; Holt, 1957; Muth, 1960; Winters, 1960; Brown and Meyer, 1961; Brown, 1962; Pegels, 1969). These forecasting techniques are advantageous due to simplicity but disadvantageous due to ad hoc nature. Chambers et al. (1971, 1974) and Makridakis and Hibon (1979) gave comprehensive analysis of several smoothening techniques across multiple time series.

Integrating the literature on existing forecasting techniques, Box et al. (1970) formulated Auto Regressive Moving Average (ARMA) models otherwise known as Box and Jenkins models. In the field of hydrology, Box and Jenkins models have been used for time series modeling of varied research interests some of which are Yevjevich (1972), Hipel et al. (1977), McLeod et al. (1977), Pegram et al. (1980), Salas et al. (1980), Loucks et al. (1981), Stedinger and Vogel (1984), Hosking (1984), Bras and Rodríguez-Iturbe, 1985, Stedinger et al. (1985), Baker (1990), Worrall et al. (2003) and Han et al. (2013). Toth et al. (2000) made a comparative analysis among ARMA model and ANN in obtaining real time flood forecast information. Keskin et al. (2006) developed a streamflow prediction model based on adaptive neural based fuzzy inference system coupled with ARMA model. Mohammadi et al. (2006) implemented goal programming for estimating parameters of ARMA model and used the developed method for river flow forecasting. However ARMA technique models only linear and stationary processes which would be a limitation in case of non-stationary and non-linear time series analysis. Apart from Box and Jenkins models, numerous other forecasting techniques have been developed along with their advancements with applications in the field of hydrology. Chang et al. (2007) and Chen et al. (2013) developed methodologies using Artificial Neural Networks (ANNs) for performing multi time steps ahead flood forecasting. Chen and Chang (2009) formulated a hybrid ANN genetic algorithm model and checked its applicability to reservoir streamflow time series. Franchini et al. (2011) have used Muskingum–Cunge routing models for real time streamflow forecasting. Asefa et al. (2006) and Lin et al. (2006) used Support Vector Machines (SVM)

* Corresponding author. Tel.: +91 80 2293 2666; fax: +91 80 2360 0404.
E-mail address: nagesh@civil.iisc.ernet.in (D. Nagesh Kumar).

0022-1694/$ - see front matter © 2013 Elsevier B.V. All rights reserved.
http://dx.doi.org/10.1016/j.jhydrol.2013.08.030

for prediction of discharge time series. Preis and Ostfeld (2008) formulated a coupled model tree-genetic algorithm scheme for the prediction of flow and water quality load in watersheds.

Consider a time series which is decomposed by some means to component time series that act as building blocks for time series. It had been observed in several works (Armstrong, 1989; Temraz et al., 1996; Zou and Yang, 2004; Gulhane et al., 2005; Hibon and Evgeniou, 2005) that when these components were modeled independently to forecast the future components and finally reconstruct the forecasted components to arrive at the required future time series, the quality of predictions was better, although the method of decomposition was empirical in nature. Anderson (1927) discussed about decomposing a time series into a number of components in which noise was discussed in an intuitive manner. A method of extracting cyclic and trend components from a time series was formulated by Frisch (1931). The presently known procedure of time series decomposition was introduced by Macaulay (1931). Wavelets (particularly Discrete Wavelet Transform (DWT)) and Empirical Model Decomposition (EMD) are two methods that can decompose non-stationary and non-linear data into a set of simpler components, which could be modeled easily. Applying the idea of modeling the decompositions, these two techniques are used to obtain components that are later used for standard time series analysis.

The objective of this study is to assess the predictability of wavelet coupled and Empirical Mode Decomposition (EMD) coupled Auto Regressive Moving Average (ARMA) models in forecasting non-stationary hydrologic data. In both the scenarios, wavelets and EMD are used to decompose a time series into simpler components to which candidate ARMA models are fitted that calibrate and predict each component independently. Finally the component predictions are combined (added) to obtain time series forecast. US Monthly streamflow volume data of four sites and IMD gridded rainfall data of two sites are considered for this study. The analysis is run to obtain two kinds of predictions one six steps ahead forecast, and two twelve steps ahead forecast. The theory regarding wavelets and EMD is presented first (in Sections 2 and 3) followed by data description and decomposition algorithms used for the analysis. The paper is concluded with discussion about the applicability of the method with non-stationary data and possible future directions in this area.

2. Wavelets

Most of the hydrologic data are non-stationary in nature (Milly et al., 2007). Such a non-stationary time series consists of events occurring for varying durations which can be ascertained through time segmentation. On the other hand, identifying periodicities that are responsible for occurrence of events in a particular data, involves segmentation in the frequency domain. Fourier analysis and the associated spectrum analysis developed by Wiener (1949) have become important tools in analyzing stationary time series. However, these methods rely on a notion of frequency that cannot accommodate time domain, loosing importance of instantaneous frequency (Boashash, 1992). This difficulty has come up due to the fact that time and frequency are canonically conjugated which is addressed for the first time by Heisenberg (1925) in the context of quantum mechanics under the principle of uncertainty. In the present case, the problem of uncertainty arises due to the fact that if resolution in the time domain is increased, resolution in the frequency domain has to be compromised and vice versa. So, to address non-stationarity, simultaneous information about time and frequency is required which was later attempted through Window Fourier Transform (WFT) (Nawab and Quatieri, 1988). The backdrop of WFT lies in its emphasis on either low frequency events (good frequency resolution) or noise (high frequency) at an instant. This is because of existence of single analysis window that remains constant during transform due to which only one kind of information is obtained. Intuitively, noise needs good time resolution (ability to identify noise by trying to narrow down on time axis) and low frequency events need good frequency resolution (ability to separate frequencies more accurately). Only when this is achieved, complete knowledge of the time series can be attained. Hence, there is necessity to consider both low frequency as well as high frequency events simultaneously which ultimately led to the concept of wavelets.

Wavelets have evolved out of two main drawbacks of Fourier analysis, infinite domain of sine and cosine waves and lack of time–frequency localization. Unlike sine and cosine waves, wavelets are localized by nature and are of discrete length, driven by two parameters translation and dilation. Through these parameters, time frequency localization property is achieved by adjusting the widow automatically for low and high frequencies giving importance to every frequency that one needs to extract. In this context, a wave shown in Fig. 1a is an oscillating periodic function of time whereas a wavelet, as in Fig. 1b shows the localized property making it a localized wave.

Fig. 2 explains the flexibility of wavelets over WFT in time frequency plane. In case of WFT (Fig. 2a), at a particular time segment, width of window is constant all over the frequency axis whereas in case of wavelet transform (Fig. 2b), window width changes across frequency axis i.e., for higher frequencies, time resolution is getting improved and vice versa indicating time frequency localization.

Due to aforementioned advantages, wavelets came into popularity in recent years in various fields. The first usage of wavelet transform was proposed by Haar (1910) although the concept of wavelets did not exist at that time. The theory was conceptualized in 1981 by Morlet et al. (1982). The term 'wavelet' was introduced by Grossmann and Morlet (1984). Meyer (1985) constructed second wavelet called Meyer wavelet other than Haar wavelet which was the only one in use till then. Mallat (1987) developed the concept of multi resolution analysis. The wavelet function that is used in any analysis is basically called as 'mother' wavelet (Heil and Walnut, 1989). Once a function satisfies a set of admissibility criteria (Daubechies, 1988), it is eligible as a mother wavelet.

With the improvements of Daubechies (1988) and Mallat (1989a,b,c), wavelets have been implemented in varied fields such as wave propagation, signal processing, geophysics, marketing and biology (Yu et al., 2013; Zheng et al., 2013; Papademetriou et al., 2013; Wang and Gupta, 2013). Daubechies (1992) and Rao and Bopardikar (1998) are some of the books that provided lucid explanation on the theory of wavelets. Coming to applications of wavelet in hydrology, Almasri et al. (2008) formulated an approach to test existence of trends using wavelets and applied it to temperature data in Sweden. Xiao-jie et al. (2008), Adamowski et al. (2009) and Sang et al. (2012a) worked on wavelet based trend identification in hydrologic time series. Duport et al. (1996) implemented wavelets to merge panchromatic and multispectral data. Galford et al. (2008) demonstrated the stability of wavelets over large extent of MODIS time series to determine expansion of row-crops and intensification of the number of crops grown in Brazil. Labat (2005) and Sang (2012) made a comprehensive review of applications of wavelet analysis in the field of hydrology.

Similar to Fourier analysis, wavelet transforms defined in continuous and discrete domains are called as Continuous Wavelet Transform (Grossmann and Morlet, 1984) and Discrete Wavelet Transform respectively. Since the present study uses the later type of transform, only that part has been discussed further.

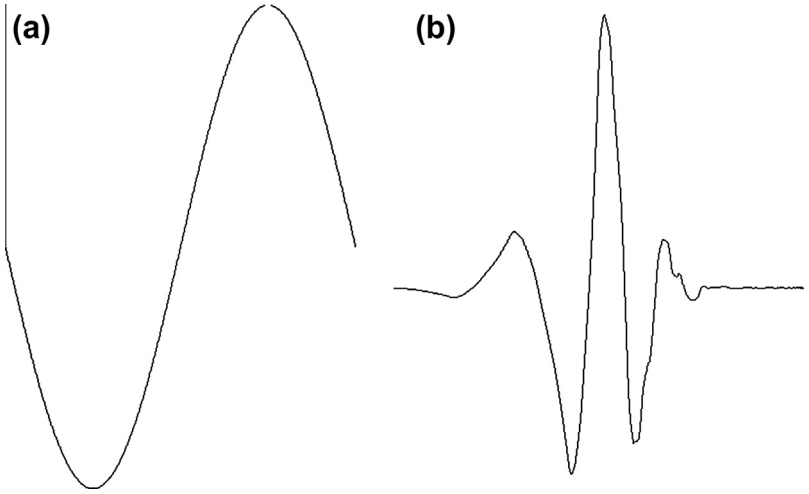

Fig. 1. Plot of (a) wave and (b) wavelet.

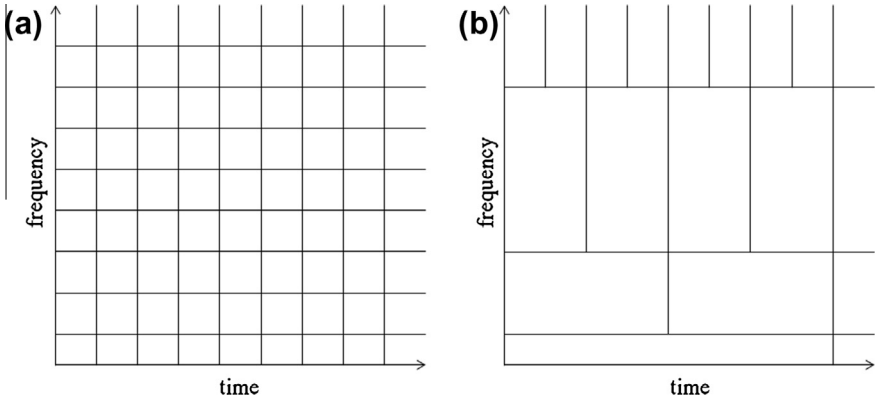

Fig. 2. Time frequency localization of (a) WFT and (b) wavelet transform.

2.1. Discrete Wavelet Transforms (DWT)

DWT is used specially for discrete datasets (Daubechies, 1992; Weng and Lau, 1994). The DWT choose such a subset of translation and location parameters with which the calculations are made, so that subsequently, discrete wavelet coefficients can be obtained which represent the minimum number of components that are needed to reflect the time series according to the mother wavelet used. Let $x[t]$ be a discrete time series of N observations $1, 2, \ldots, N$.

The discrete wavelet function is represented by

$$\psi_{u,v}(t) = \frac{1}{\sqrt{2^u}}\psi\left(\frac{t - v2^u}{2^u}\right) \tag{1}$$

where 2^u is the scale parameter; $v2^u$ is the translation parameter $(u, v \in \mathbb{Z})$; v is the location index $(1 < v < 2^{-u}N)$ that indicates the nonzero portion of wavelet function in the normalizing factor $2^{-u/2}$; u indicates the level of decomposition. Here the discretisation is achieved by implementing the factor 2^u in actual wavelet function (Eq. (2)). During this, the consecutive values of discrete scales as well as corresponding sampling intervals differ by the factor 2 the process of which is called dyadic sampling (Rao and Bopardikar, 1998). DWT coefficients of $x[t]$ are obtained from

$$x''_{u,v} \equiv x''(2^u, v2^u) = \int_{-\infty}^{\infty} x[t]\frac{1}{\sqrt{2^u}}\psi^*\left(\frac{t - v2^u}{2^u}\right)dt \tag{2}$$

Inverse Discrete Wavelet Transform can be applied to reconstruct the time series from wavelet coefficients $x''_{u,v}$ (Daubechies, 1992; Rao and Bopardikar, 1998) using

$$x[t] = \sum_{u=-\infty}^{\infty}\sum_{v=-\infty}^{\infty} x''_{u,v}2^{-u/2}\psi\left(\frac{t - v2^u}{2^u}\right) \tag{3}$$

As scale and decomposition level are decreased, the coefficients are more localized in time resolution and hence high frequency components can be identified whereas when they are increased, the coefficients are more localized in frequency resolution and hence low frequency events can be accessed. This process requires multi resolution analysis of the data.

2.2. Multi Resolution Analysis (MRA)

The idea of MRA is to extract the resolutions in time domain from finer scale to coarser scale using different dilates and translates of the mother wavelet under study. Dilates (scale parameter) switches the resolutions while translates (location parameter) apply a particular scale parameter throughout the time series. Martínez and Gilabert (2009) studied Normalized Difference Vegetation Index (NDVI) time series using MRA to capture and describe intra and inter annual changes in the data. Recently, considerable work has been undertaken in fusion of wavelets with other techniques to model a time series such as wavelet neural networks (Wang and Ding, 2003; Nourani et al., 2009; Adamowski and Chan, 2011; Wei et al., 2013), wavelet neuro fuzzy conjunction model (Partal and Kişi, 2007; Kişi and Shiri, 2011) and wavelet support vector machine conjunction model (Kişi and Cimen, 2011). DWT is implemented in a pyramid algorithm (Mallat, 1989b; Vishwanath, 1994; Tan et al., 2011) to perform MRA (Kumar and Foufoula-Georgiou,

1993; Rao and Bopardikar, 1998; Bayazit and Aksoy, 2001), which takes into account its representation at multiple resolutions of time and frequency. Intuitively, in a pyramid algorithm, wavelet translates along finest resolution, filters out that corresponding component, goes to next finer resolution, translates along, and filters out that component. This process continues depending upon the number of levels to which the time series has to be decomposed. MRA achieves the decomposition by using the concept of filter banks associated with mother wavelet. A filter bank is called two band filter bank in MRA since it consists of two sets of filters (Tay and Kingsbury, 1993). One band is for decomposing (called the analysis phase) the time series and the other is for reconstructing the time series (called the synthesis phase). Being a multi resolution analysis, each band of filters has two filters; low pass filter (α) and high pass filter (β) [Table 1] of which α captures low frequency which is termed as approximation (A) and β captures high frequency component termed as detail (D).

The application of filter to the time series is influenced by two steps (1) time series extension and (2) convolution of filter with extended time series. When convolution is carried out on an unmodified finite time series, at the ends (boundaries) of the series, convolution may not be computed since the values next to the boundaries are not defined (de Queiroz, 1992; Cohen et al., 1993). So, in order to overcome this problem, time series is extended using time series extension methods (Strang and Nguyen, 1996) on either of the ends (step 1) and then step 2 is carried out. Finally, values that are concerned with filter and original time series are selected. Five time series extension methods are used in the present study and the method producing best forecasts is selected. To demonstrate how the extensions are made, a sample time series $x = 1, 2, 3, 4, 5$ (Fig. 3a) is taken and extended using these techniques (Fig. 3b–f).

Table 1
Two band filter bank in MRA.

Filter	Phase	
	Analysis/decomposition	Synthesis/reconstruction
Low pass	α^d	α^r
High pass	β^d	β^r

(1) Symmetric Extension (half-point) – sym.
(2) Symmetric Extension (whole-point) – symw.
(3) Anti-Symmetric Extension (half-point) – asym.
(4) Anti-Symmetric Extension (whole-point) – asymw.
(5) Simple constant extrapolation – sp0.

These methods are developed to only reduce to certain extent the effect of boundaries on time series on application of filter. They do not completely eradicate the problem at boundaries.

During the decomposition phase, the two time series obtained from filter application will have redundant information (Strang and Nguyen, 1996). This situation is monitored by having only half of the series that come out of filter application, by the process called downsampling by the factor 2 which involves retaining only the even indexed values in a time series. During synthesis phase, the downsampled components are upsampled which involves filling in zeros at odd indices to attain the length of the time series. In these processes, filter application is done using convolution. The following sections give an overview of convolution, downsampling and upsampling processes.

2.3. Convolution

Consider two time series $\{f_t: t = 1, 2, \ldots, i\}$ and $\{g_t: t = 1, 2, \ldots, j\}$ of length i and j respectively. Convolution of f and g yields vector h of length $i + j - 1$ from the following equation.

$$h_t = f * g = \sum_k f_k g_{t-k+1} \tag{4}$$

where k ranges from $\max(1, t + 1 - j)$ to $\min(t, i)$. Further information regarding convolution, is available in Strang and Nguyen (1996).

2.4. Downsampling and upsampling

Let $\{e_t: t = 1, 2, \ldots, n\}$ denote a time series. Downsampling of e_t is achieved by using operator $\delta: (x_1, x_2, x_3, x_4, x_5, x_6, \ldots) \rightarrow (x_2, x_4, x_6, \ldots)$

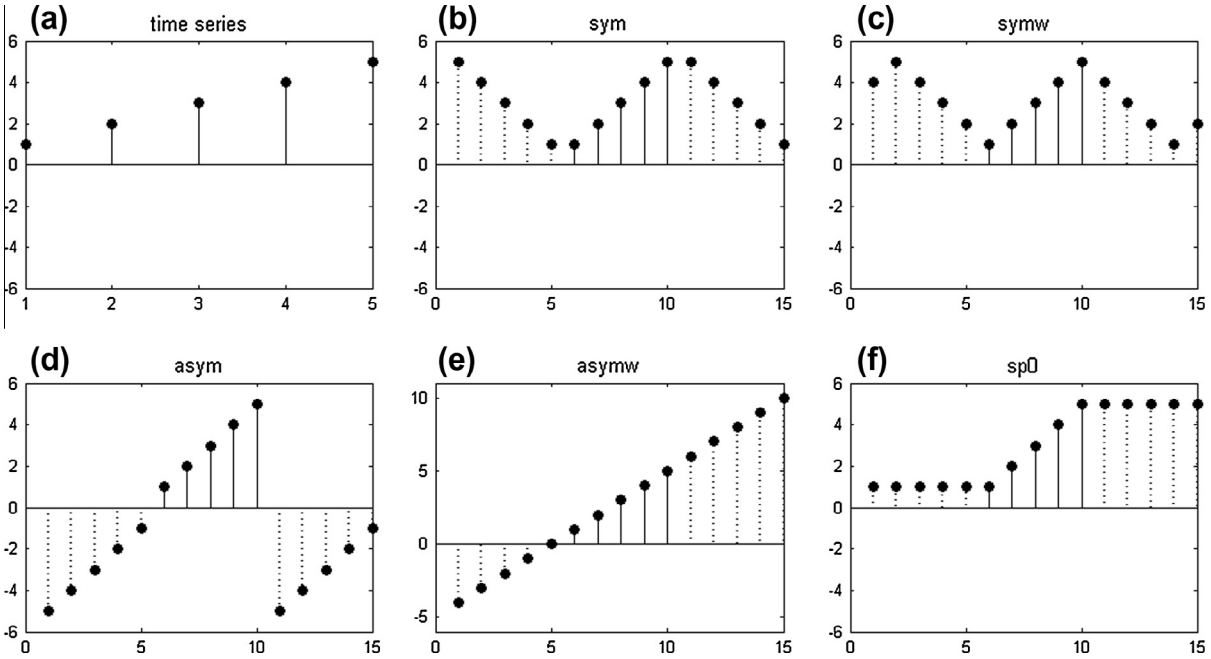

Fig. 3. Time series extension methods.

and upsampling of e_t is carried out by using operator U: $(x_1, x_2, x_3, x_4, \ldots) \rightarrow (0, x_1, 0, x_2, 0, x_3, 0, x_4, 0, \ldots)$ resulting in following equations.

$$[\delta(e)]_k = \{e_k : k = 2, 4, 6 \ldots\} \tag{5}$$

$$[U(e)]_k = \begin{cases} e_{k/2}, & k \text{ is even} \\ 0, & k \text{ is odd} \end{cases} \tag{6}$$

Coming to mother wavelet, nearly fifteen families of mother wavelets are available in literature (Misiti et al., 1996), some of them are Daubechies family (Daubechies, 1992), Symlets (Misiti et al., 1996), Coiflets (Daubechies, 1992), Biorthogonal wavelets (Chui, 1992), etc. In present implementation, Daubechies 5 (db5) mother wavelet is used. Fig. 4 shows db5 mother wavelet along with corresponding decomposition and reconstruction filter banks of the wavelet.

Considering the mother wavelet and the number of levels of decomposition selected, the following algorithm explains decomposition of the time series into components that are of length equal to that of the time series.

2.5. Algorithm of time series decomposition using DWT

(1) Let $\{x_t \in \mathbf{x}: t = 1, 2, \ldots, n\}$ denote a time series. Let η denote number of levels of decomposition.
(2) Select mother wavelet W and the kind of extension method to apply over $\mathbf{x}$. Let the selected wavelet's filters be assigned notations followed in Table 1.
(3) Compute approximation A'_1 and detail D'_1 using the Eqs. (7) and (8) respectively which involves convolution operation (Eq. (4))

$$A'_1 = \mathbf{x} * \alpha^d \tag{7}$$

$$D'_1 = \mathbf{x} * \beta^d \tag{8}$$

(4) Downsample A'_1 and D'_1 to A''_1 and D''_1 (level one approximation and detail coefficients) by using the downscaling operator described in Eq. (5). The modified approximation (A''_1) and detail (D''_1) coefficients are as follows.

$$A''_1 = [\delta(A'_1)]_t = \{A^d_{1,t} : t = 2, 4, 6, \ldots\} \tag{9}$$

$$D''_1 = [\delta(D'_1)]_t = \{D^d_{1,t} : t = 2, 4, 6, \ldots\} \tag{10}$$

For a η level decomposition, steps 1–4 are carried out for η iterations (maintaining constant W and extension method) by taking approximation A''_q (q – iteration number) from step 4 (Eq. (9)) as $\mathbf{x}$ for the next iteration. So, for a 3 level decomposition, A''_1 obtained at the end of first iteration is taken as $\mathbf{x}$ for the second iteration and A''_2 obtained at the end of second iteration is taken as $\mathbf{x}$ for the third iteration which results in final approximation A''_3. At the end of each iteration, corresponding details (obtained from Eq. (10)) are preserved. Finally, a η level decomposition results in η number of details $(D''_1, D''_2, D''_3, \ldots, D''_\eta)$ and one approximation (A''_η).

(5) Upsample coefficients $(D''_1, D''_2, D''_3, \ldots, D''_\eta, A''_\eta)$ to $(D^*_1, D^*_2, D^*_3, \ldots, D^*_\eta, A^*_\eta)$ using upsampling operator described in Eq. 6. This modifies approximation and details as follows

$$A^*_\eta = \left[U\left(A''_\eta\right)\right]_k = \begin{cases} A''_{\eta,k/2}, & k \text{ is even} \\ 0, & k \text{ is odd} \end{cases} \tag{11}$$

$$D^*_q = [U(D''_q)]_k = \begin{cases} D''_{q,k/2}, & k \text{ is even} \\ 0, & k \text{ is odd} \end{cases}, \quad q = 1, 2, \ldots, \eta \tag{12}$$

(6) Compute A^{**}_η and D^{**}_q from (A^*_η, D^*_q) and (α^r, β^r) using following equations.

$$A^{**}_\eta = A^*_\eta * \alpha^r \tag{13}$$

$$D^{**}_q = D^*_q * \beta^r, \quad q = 1, 2, \ldots, \eta \tag{14}$$

(a) Reconstruct A^{**}_η to the length n by repeating steps 5–6 (Eqs. (11) and (13)) for η times resulting in obtaining the completely reconstructed approximation A_η.
(b) Reconstruct D^{**}_q to the length n by repeating steps 5–6 (Eqs. (12) and (14)) for q times during which for the last $(q-1)$ iterations, Eq. (16) is modified as $D^{**}_q = D^*_q * \alpha^r$. In both processes, the coefficients obtained at the end of each iteration are given as input time series at the initiation of next iteration. This step obtains a set of completely reconstructed

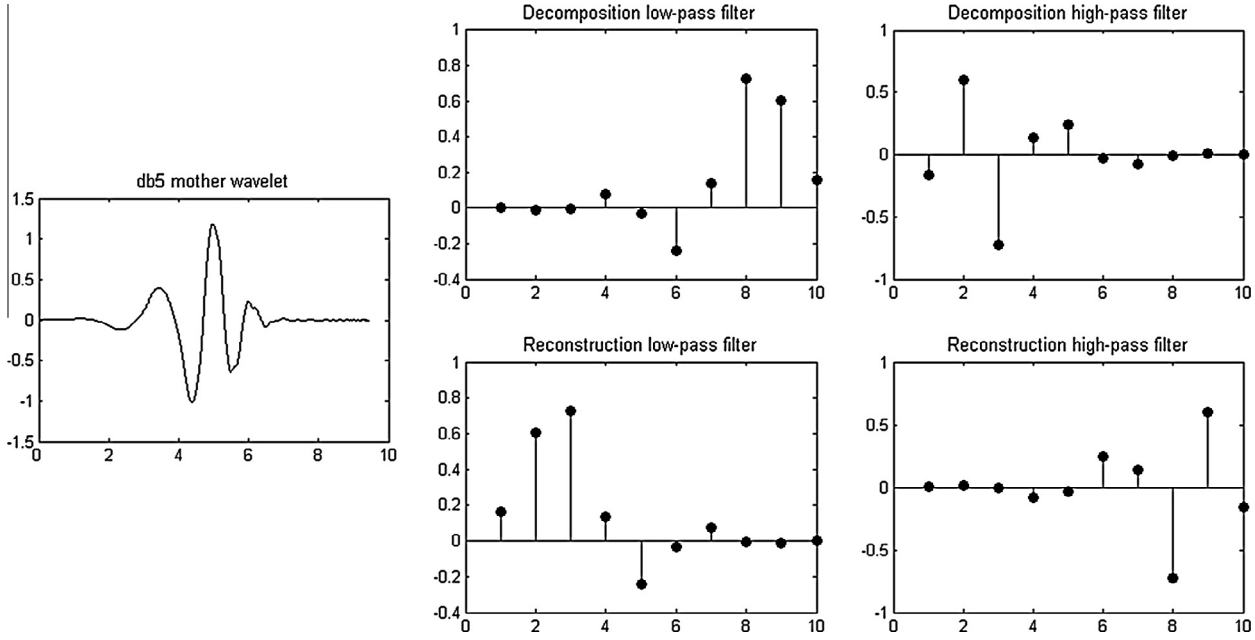

Fig. 4. Daubechies (db5) mother wavelet along with its decomposition and reconstruction filter banks.

components $D_1, D_2, D_3, \ldots, D_\eta, A_\eta$ which are of length n. The summation of these components yields original time series (Eq. (15)).

$$x_t = A_\eta + \sum_{q=1}^{\eta} D_q \tag{15}$$

3. Empirical Mode Decomposition

Empirical Mode Decomposition (EMD) is a non-stationary data analysis technique (Huang et al., 1998; Magrin-Chagnolleau and Baraniuk, 1999; Huang and Wu, 2008). It is developed out of the fact that most of the time series in nature contain multiple frequencies leading to existence of different scales simultaneously. Application of EMD has picked up pace in the field of hydrology due to its simplicity and lesser computational cost. Sang et al. (2012b) used EMD along with the concepts of entropy to identify periods in hydrologic time series. Lee and Ouarda (2012) simulated non-stationary oscillations using EMD and nonparametric simulation techniques. McMahon et al. (2008) devised a new approach to generate rainfall sequences considering climatic phenomena using EMD. Napolitano et al. (2011) discussed the aspects of artificial neural network in hindcasting of daily stream flow data through EMD. The method works in successively extracting these scales from the time series in the form of Intrinsic Mode Functions (IMF). An IMF by definition has to satisfy two conditions:

1. The difference between the number of local extremes and zero-crossings must be zero or at most differ by one with the function being symmetric in time.
2. At any point, the mean value of the envelope, defined by local maxima as well as that of envelope defined by local minima must be zero.

This intuitively means that an IMF is obtained by eliminating the effect of various locally occurring amplitude and frequency modulations and eliminating asymmetries in corresponding time series with respect to the zero level. Similar to the effect of boundary distortion that occurs with wavelets, EMD also experiences boundary effects. So, Huang et al. (1998) extended original time series by appending artificial time series (called characteristic waves) on both the boundaries. These characteristic waves are constructed by many methods. Important of them are either by repeating the implicit mode derived from extreme values at boundaries or by extending either symmetrically or periodically at boundaries. For the present study, only symmetric extension is used as extension method since it is observed that the results have not varied much due to change of extension methods.

EMD performs the decomposition of time series into IMFs by an iterative procedure called 'sifting' explained in the following algorithm.

3.1. Algorithm of time series decomposition using EMD

(1) Let $\{z_t \in \mathbf{z}: t = 1, 2, \ldots, n\}$ denote a hydrologic time series that will be input to the sifting process.
(2) Extract all the local extremes in $\mathbf{z}$. Use an interpolation technique to connect all local maxima and minima to obtain upper and lower envelopes respectively. Generally a cubic spline interpolation (Hou and Andrews, 1978) is employed (Rilling et al., 2003; Huang and Wu, 2008).
(3) Find difference between $\mathbf{z}$ and mean of two envelops resulted in step 2 to obtain first sub time series p ($p = \mathbf{z} - envelop's\ mean$).
(4) p is checked against IMF criteria which, if not met, steps 1–3 are iterated by substituting p as $\mathbf{z}$ and the process is repeated until the resulting time series satisfies the criterion.
(5) Make final sub series p (resulting from step 4) as I_j, the jth IMF, and the resulting residue as R_j ($R_j = R_{j-1} - I_j$, where $R_0 = \mathbf{z}$).
(6) Repeat steps 1–5 for N times, by initializing residue time series R_j as $\mathbf{z}$ until final residue series R_N becomes monotonic by nature. The original time series can therefore be expressed as (Eq. (16))

$$z(t) = \sum_{j=1}^{N} I(t)_j + R(t)_N \tag{16}$$

4. Data

In order to test the methodologies of wavelet and EMD based time series algorithms, monthly total streamflow volume and monthly total rainfall data are used in the study. Streamflow data is collected from USGS Hydro-Climatic Data Network (HCDN) CD-ROM (Slack and Landwehr, 1994) consisting of 1659 sites of streamflow records spread throughout United States, cumulatively spanning for the period 1874–1988. Out of this, 1273 sites were found to have continuous record which could be used for time series analysis. For the present study, only data with continuous record are considered although sites with missed data can also be modeled using data filling techniques (Simonovic, 1995; Starrett et al., 2010; Elshorbagy et al., 2002). Since the aim of the study is to analyze the performance of wavelets and EMD in forecasting when the data is non-stationary, KPSS test (Kwiatkowski et al., 1992) was performed on the selected 1273 sites. The results indicated that for 489 streamflow records, the assumption of stationarity is rejected at 95% confidence levels. The forecasting algorithms presented in Sections 5 (wavelet) and 6 (EMD) were applied to the selected records. For brevity, results pertaining to four streamflow locations have been presented based on varied properties of the data. Table 2 presents the criteria of site selection along with reason behind the selection. Details of selected sites along with their statistical properties are given in Table 3.

Monthly total rainfall data prepared from $0.5^\circ \times 0.5^\circ$ resolution, Indian Meteorological Department (IMD) daily gridded rainfall data of Indian subcontinent over a period of 1971–2005 (Rajeevan and Bhate, 2009) is used. It is observed that 1149 grid locations fall in India. KPSS stationarity test is applied to the records at these locations to discriminate stationary and non-stationary grid records. It is found that for 170 grids records the assumption of stationarity is rejected at 95% confidence level and these only are considered for the present study. The forecasting algorithms presented in Sections 5 (wavelet) and 6 (EMD) were applied to these 170 grid locations. For brevity, results pertaining to two grid locations, from the state of Karnataka, are only presented in the current study. The details of the rainfall locations are shown in Table 4.

4.1. Selection of candidate models for time series analysis

The number of candidate models affects the computational efficiency of any forecasting technique. Although considerable research has been done in the area of developing model selection criteria (Akaike, 1974, 1978; Rissanen, 1978; Schwarz, 1978; Hannan and Quinn, 1979; Shibata, 1980; Voss and Feng, 2002; Seghouane and Bekara, 2004), none of the works gave a directive in selecting the upper limit for restricting the population of candidate models which makes them uncertain. Order selection can be made

Table 2
Site selection criteria.

S.No	Property	Sites	Remarks
1	Greater record length	1	Have proportionately more peaks to be predicted
2	Minimum record length	2	Check if wavelets and EMD could predict with lesser record lengths
3	Coefficient of variation between 1 to 2 ($1 \leqslant C_v \leqslant 2$)	3, 4	Accuracy of predictions in high variability conditions could be accounted to predictability of model in case of rainfall

Table 3
Details of selected streamflow sites.

Site	Name (ID)	Lat.	Lon.	Length (years)	Mean ($\times 10^5$ m^3)	Std. Dev. ($\times 10^5$ m^3)	C_v
1	Mississippi River at Clinton (05420500)	41°46′50″	90°15′07″	115	35636.93	22465.53	0.64
2	North Fork River near Tecumseh (07057500)	36°37′23″	92°14′53″	44	542.97	393.65	0.73
3	War Eagle Creek near Hindsville (07049000)	36°12′02″	93°51′20″	18	207.32	288.99	1.39
4	Lopez Creek near Arroyo Grande (11141280)	35°14′08″	120°28′17″	21	8.23	14.83	1.80

Table 4
Details of selected rainfall sites.

Site	Lat. (°)	Lon. (°)	Length (years)	Mean (mm)	Std. Dev. (mm)	C_v
5	14	75	35	180.33	345.75	1.92
6	16	75	35	53.64	79.44	1.48

based on Auto Correlation (AC) and Partial Auto Correlation (PAC) curves in case of either pure AR or MA processes. Fig. 5 presents sample AC and PAC for streamflow site Mississippi River at Clinton, IA (site 1) and rainfall site 5.

It is observed that, in both the sites, numerous significant lags have occurred both in AC and PAC plots which results in neither pure AR nor pure MA processes leading to the ARMA models. Since, number of significant lags is very high, with respect to principle of parsimony, orders up to ARMA (6,4) are considered as candidate model population. Model selection is based on minimum mean square error criterion (Kashyap and Rao, 1976).

The component time series obtained on using decomposition algorithm are modeled using standard ARMA models by Box et al. (1970).

Fixing the number of levels of decomposition largely controls the size of computational effort in this case of wavelet analysis. For a time series of length n, Daubechies (1992) stated that the maximum number of decompositions can be taken as $\log_2 n$.

Based on this formula, the maximum number of levels obtained for the longest site data (site 1) is 11. Although Sang et al. (2010) proposed a methodology of finding optimum number of decompositions using wavelet energy entropy and Mote Carlo simulations,

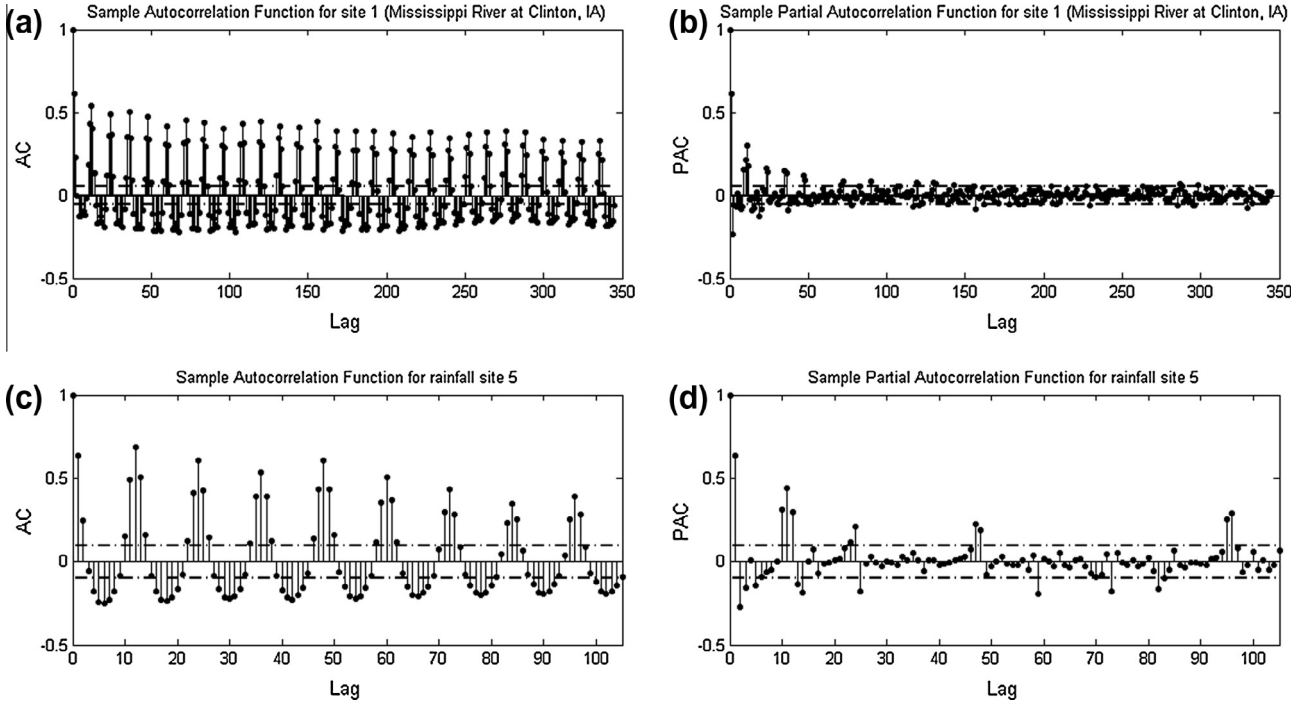

Fig. 5. Autocorrelation (AC) and Partial Autocorrelation (PAC) plots for streamflow site Mississippi River at Clinton, IA (a and b) and rainfall site 5 (c and d).

they have concluded that the method was developed in the context of de-noising and also it has to be tested on varied datasets. Since the approximation time series gets smoother as the decomposition level is increased, it is observed that the amount of information carried by the time series is decreasing. According to this notion, wavelet decomposition algorithm is carried out for all the non-stationary streamflow as well as rainfall sites (489 streamflow sites and 170 rainfall locations, totaling 659 sites) from 1 to 11 decompositions and at every site for every decomposition, corresponding approximation is used to calculate percentage variance ratio $V_{i,dec}$ (Eq. (17)).

$$V_{i,dec} = \frac{\mathrm{var}(A_{i,dec})}{\mathrm{var}(data_i)} * 100, \quad i = 1,2,\ldots,659, \quad dec = 1,2,\ldots,11 \tag{17}$$

where $\mathrm{var}(A_{i,dec})$ is the variance of approximation of ith site and dec decomposition level; $\mathrm{var}(data_i)$ is the variance of data at ith site. Fig. 6 gives plots of average percentage variance ratio and average performance of all the sites.

It can be seen from average percentage variance ratio plot that the amount of variance explained is depleting, with increase in number of decompositions. At one level decomposition, most of the information from time series is retained in approximation (84.6%) which cannot be ignored. Also, beyond 10 levels, less than 1% of variance ratio is explained by corresponding approximation which does not possess important information. So, based on this observation, upper and lower limits for all the sites are fixed as ten and one.

4.2. Performance measures

For the present study, two measures Normalized Root Mean Square Error (*NRMSE*) (Eq. (18)) and Nash–Sutcliffe Efficiency Index (E_f) (Eq. (19)) are used.

$$NRMSE = \frac{RMSE}{x_{\max} - x_{\min}} = \frac{\sqrt{\frac{\sum_{i=1}^{n}(y_i - x_i)^2}{n}}}{x_{\max} - x_{\min}} \tag{18}$$

where $x_{\max}$, x_{mim} are maximum, minimum of observed values; y_i, x_i are actual and predicted values of output; n is the number of values. *NRMSE*, is the normalized version of *RMSE*. Eq. (18) depicts that *RMSE* is normalized with reference to the range of observed values to control the range of error outcomes. An *NRMSE* value of greater than 1 means that the average root of squared deviation of predicted values from the observed (numerator) is greater than the range of observed values (denominator) suggesting poor model performance. Ideally the error value should be 0. The equation of *NRMSE* stated above need not be taken as standard since the normalization could be carried out by any other means (maximum observed value, mean, etc.) according to necessity.

To measure goodness of fit of any model calibration, traditionally, the correlation coefficient was used despite its theoretical applicability to only linear models having an intercept. The Nash–Sutcliffe Efficiency Index or coefficient of Efficiency provides an indication of how the predictions of model are carried out away from mean which means that this measure could be used to comment on model capabilities at extremes. Closer the E_f value to 1, better the network fit. E_f is given by

$$E_f = 1 - \frac{\sum_{i=1}^{n}(y_i - x_i)^2}{\sum_{i=1}^{n}(y_i - \bar{y})^2} \tag{19}$$

where y_i and x_i are actual and obtained values of output; $\bar{y}$ is the mean of actual output values; n is the number of values. E_f values can range from $-\infty$ to 1. A value of 1 corresponds to 100% accuracy of predicted values with reference to the observed, whereas 0 indicates that the model predictions are equal to mean of the observed values, whereas $E_f < 0$ occurs when the variance explained by residuals is greater than that of observed data which indicates poor performance of model.

The following algorithms (Sections 5 and 6) provide an account of calibration and validation of wavelet based time series analysis as well as EMD based time series analysis methodologies.

5. Wavelet based time series analysis

(1) Let $\{y_t \in \mathbf{y}: t = 1, 2, \ldots, n\}$ denote a hydrologic time series. Select wavelet function W and decide candidate ARMA models to be used for analysis. Let the number of models selected be Λ. Divide time series into calibration and validation datasets. Let them be $\mathbf{y_{calib}}$(80 of $\mathbf{y}$) and $\mathbf{y_{valid}}$(20 of $\mathbf{y}$) respectively. Calibration data is divided into $\mathbf{y_{calib,1}}$ (75% of $\mathbf{y_{calib}}$) and $\mathbf{y_{calib,2}}$ (25% of $\mathbf{y_{calib}}$). Let the range of decompositions be η_s, where $s = [1, 10], s \in \mathbb{Z}$.

Calibration:

(2) For a decomposition level in η (where $\eta \in \eta_s$), subject $\mathbf{y_{calib,1}}$ to wavelet decomposition algorithm using wavelet function W selected in step 1 to obtain components $D_1, D_2, \ldots, D_\eta$, and A_η.

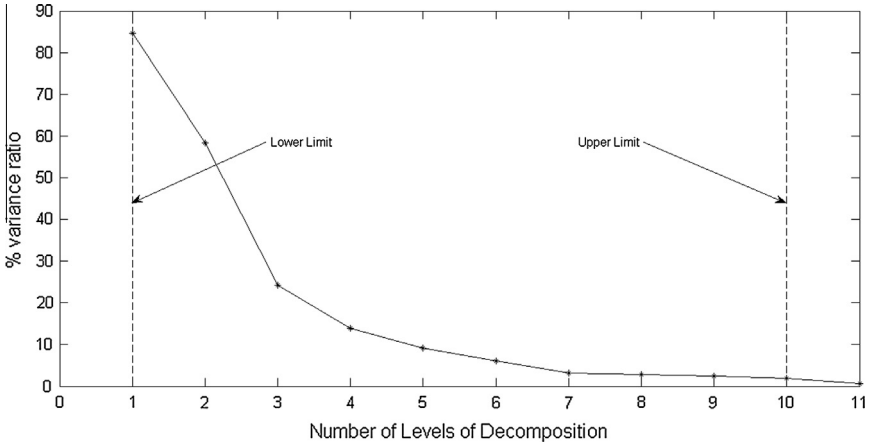

Fig. 6. Plot of average % variance ratio versus number of decompositions.

(3) Using a particular candidate model *ARMA*(p, q), compute ρ step ahead forecast across all the components which would result in component forecasts ($D^f_1, D^f_2, \ldots, D^f_\eta$, and A^f_η). Store these values.
(4) At the end of step 3, observed data record for ρ time steps is obtained. Add this data to $\mathbf{y_{calib,1}}$. Initialize the newly appended outcome as $\mathbf{y_{calib,1}}$.
(5) Repeat steps 2–4 by updating $\mathbf{y_{calib,1}}$ with the observed data obtained in step 4 until entire calibration period is covered. During every iteration, for a particular candidate model *ARMA*(p, q), ρ step ahead forecast across all the components is performed and the forecasts across components are respectively appended with previously stored components forecast (step 3) to finally obtain components forecast for complete calibration period ($D^f_{1,calib}, D^f_{2,calib}, \ldots, D^f_{\eta,calib}$, and $A^f_{\eta,calib}$).
(6) Perform steps 3–5 using all the selected candidate ARMA models. For Λ candidate models, one would obtain Λ sets of component forecasts at the end of step 5. Select best model of Λ candidate models at each component by comparing corresponding calibration forecasts (obtained from step 5) with observed components using minimum mean square error criterion.
(7) Add the forecasts across components that are obtained by using respective optimum ARMA models (from step 6) to result in ρ step ahead calibration forecast for $\mathbf{y_{calib,2}}$.
(8) Apply steps 1–7 for all the values of η_s. Compare the calibration forecasts based on minimum NRMSE criterion and select candidate decomposition models to be used for validation. A candidate η' level decomposition model has respective optimum ARMA models at each component to perform ρ step ahead prediction. For the present study, five decomposition models were selected out of ten and are used for validation. Application of decomposition model involves initially wavelet decomposition algorithm (to obtain components) and later component ARMA models (applied iteratively) to obtain ρ step ahead prediction for required time period.

Validation:

(9) Calibration data $\mathbf{y_{calib}}$ is fed to candidate decomposition models (from step 8) individually and corresponding ρ step ahead forecasts are computed. Later, for every model output, add the forecasts across components and select the best outcome by comparing it with observed data record using minimum *NRMSE* criteria.
(10) Similar to step 4, the observed data for ρ steps is appended with $\mathbf{y_{calib}}$ and step 9 is run again.
(11) Steps 9–10 are run for entire validation period and the optimum forecasts at each iteration are appended, finally forming ρ step ahead validation forecast $\mathbf{y^f_{valid}}$.

Fig. 7 explains flowchart of wavelet based time series analysis algorithm.

6. EMD based time series analysis

(1) Let $\{y_t \in \mathbf{y}: t = 1, 2, \ldots, n\}$ denote a hydrologic time series. Decide candidate ARMA models to be used for analysis. Let the number of models selected be Λ. Divide time series into calibration and validation datasets. Let them be $\mathbf{y_{calib}}$ (80% of $\mathbf{y}$) and $\mathbf{y_{valid}}$ (20% of $\mathbf{y}$) respectively. Calibration data is divided into $\mathbf{y_{calib,1}}$ (75% of $\mathbf{y_{calib}}$) and $\mathbf{y_{calib,2}}$ (25% of $\mathbf{y_{calib}}$).

Calibration:

(2) Subject $\mathbf{y_{calib,1}}$ to EMD decomposition algorithm to obtain component IMFs and residue ($I_1, I_2, \ldots, I_n$, and R_n).

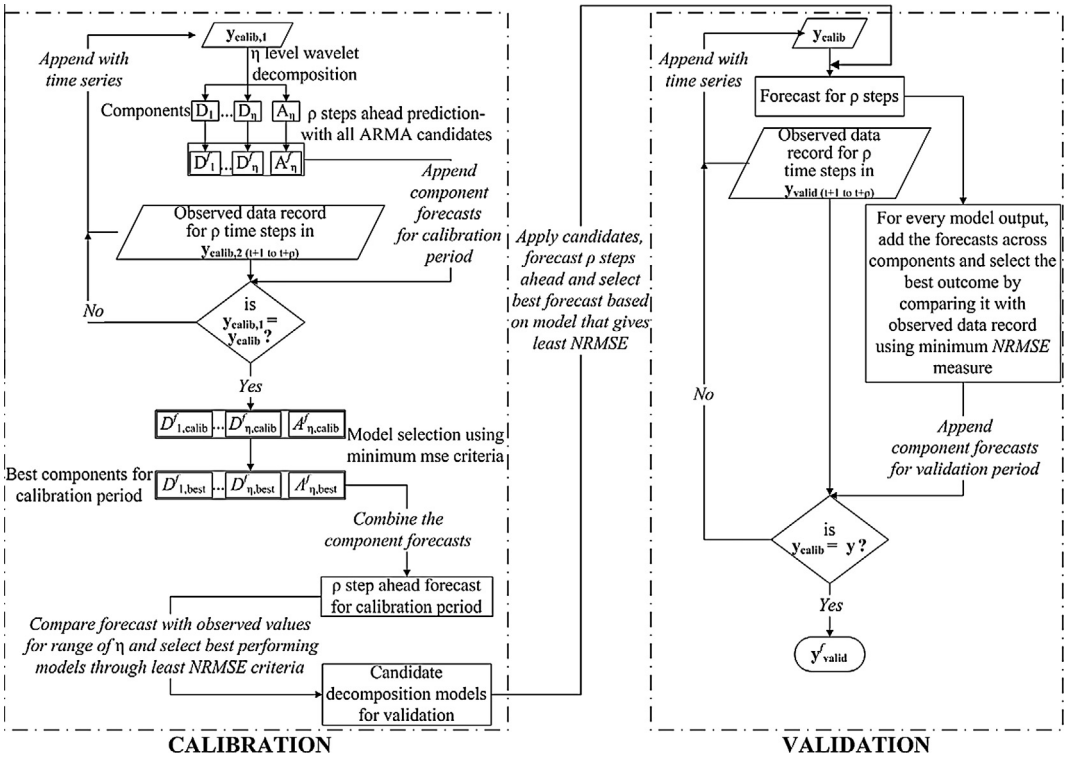

Fig. 7. Flowchart of wavelet based time series analysis algorithm.

(3) Using a particular candidate model *ARMA*(p, q), compute ρ step ahead forecast across all the components (obtained from step 2) which would result in component forecasts ($I_1^f, I_2^f, \ldots, I_n^f$, and R_n^f). Store these values.
(4) At the end of step 3, observed data record for ρ time steps is obtained. Add this data to $\mathbf{y_{calib,1}}$. Initialize the newly appended outcome as $\mathbf{y_{calib,1}}$.
(5) Repeat steps 2–4 by updating $\mathbf{y_{calib,1}}$ with the observed data obtained in step 4 until entire calibration period is covered. During every iteration, for a particular candidate model *ARMA*(p, q), ρ step ahead forecast across all the components is performed and the forecasts across components are respectively appended with previously stored components forecast (step 3) to finally obtain components forecast for complete calibration period ($I_{1,calib}^f, I_{2,calib}^f, \ldots, I_{n,calib}^f$, and $R_{n,calib}^f$).
(6) Perform steps 3–5 using all the selected candidate ARMA models. For Λ candidate models, one would obtain Λ sets of component forecasts at the end of step 5. Select best model of Λ candidate models at each component by comparing corresponding calibration forecasts (obtained from step 5) with observed components using minimum mean square error criterion.
(7) Add the forecasts across components that are obtained by using respective optimum ARMA models (from step 6) to result in ρ step ahead calibration forecast for $\mathbf{y_{calib,2}}$.
(8) Establish decomposition model from the results of step 7 which has respective optimum ARMA models at each component to perform ρ step ahead prediction. Application of decomposition model involves initially EMD decomposition algorithm (to obtain components) and later component ARMA models (applied iteratively) to obtain ρ step ahead prediction for required time period.

Validation:

(9) Calibration data $\mathbf{y_{calib}}$ is fed to decomposition model (from step 8) to result in ρ step ahead forecasts. Later, the forecasts obtained are added across components and the resulting time series forecast is stored.
(10) Similar to step 4, the observed data for ρ steps is appended with $\mathbf{y_{calib}}$ and step 9 is run again.
(11) Steps 9–10 are run for entire validation period and the optimum forecasts at each iteration are appended, finally forming ρ step ahead validation forecast $\mathbf{y_{valid}^f}$.

Fig. 8 explains flowchart of EMD based time series analysis algorithm.

7. Results and discussion

The wavelet and EMD based forecasting algorithms discussed in Sections 5 and 6 respectively are applied to four streamflow and two rainfall locations to derive six months ahead forecasts (6 MAF) and twelve months ahead forecasts (12 MAF). In all the cases, *NRMSE* is considered as criteria for model selection since the measure is obtained in a limited comparable range (due to normalization). Along with the measure of *NRMSE*, E_f also is computed between predicted and observed data to assess the ability of the model in predicting extremes of the time series.

In case of wavelet based forecasting, five time series extension methods are used (Section 2.2) since the forecasts are affected significantly at some of the sites. It has to be noted from step 8 of wavelet based algorithm (Section 5) that the forecasts for calibration period are obtained for a range of decompositions η_s which, in present study is considered to be from 1 to 10. Based on the forecasts during calibration period, out of ten models, five decomposition models are selected as candidates for validation purpose. This process is carried out on all the sites considered for the analysis. For brevity, the results pertaining to site 1 are presented for illustration in Table 5. It has to be observed that for one site, results during calibration correspond to performance of ten decomposition levels across five time series extension techniques used in the study. So, for a particular extension technique, five best performing decomposition levels were selected (with their corresponding optimum component ARMA models) using optimum *NRMSE* measure and are finally used for validation purpose.

Tables 6 and 7 present the quality of predictions for validation period obtained using measures of *NRMSE* and E_f obtained for 6

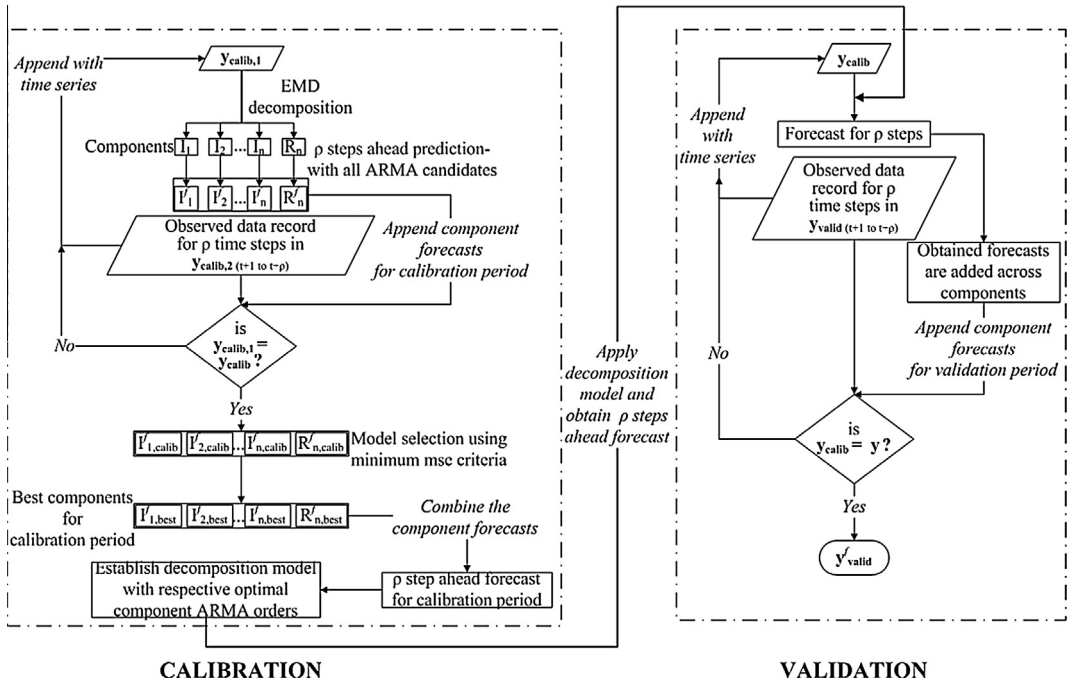

Fig. 8. Flowchart of EMD based time series analysis algorithm.

Table 5
Calibration results of site 1 represented by *NRMSE* across decomposition levels for five extension techniques used.

Exten.	Dec.									
	1	2	3	4	5	6	7	8	9	10
sym	0.94	0.84	1.02	0.99	0.94	0.93	0.92	0.90	0.90	0.90
symw	0.96	0.85	0.97	0.95	0.94	0.91	0.90	0.90	0.90	0.90
asym	0.98	1.00	1.22	1.28	1.24	1.22	1.22	1.22	1.22	1.22
asymw	0.92	0.87	1.06	1.24	1.47	1.56	1.43	2.01	2.02	3.76
sp0	0.94	0.84	0.97	0.95	0.92	0.92	0.93	0.93	0.93	0.93

MAF and 12 MAF, across six sites, and five extension methods. The best error measures in Table 6 are highlighted in bold italics. An initial study of the results from the Tables 6 and 7 signaled that the wavelet based forecasting method has performed comparatively well in predicting rainfall sites than that of streamflow sites under both of the forecasting scenarios. In the case of site 1, the optimum validation predictions are observed to perform well with *NRMSE* values of 0.81 (6 MAF) and 0.82 (12 MAF). In both the cases, effectively, sp0 extension technique is utilized. Corresponding to this extension method, at site 1, E_f values of 0.35 (6 MAF) and 0.32 (12 MAF) [Table 7] are attained. The values of E_f imply that the predictions are away from mean of the validation dataset which indicate that the method might be successful to an extent in predicting the extremes of the site 1 validation data. The outcome of site 2 predictions illustrates that the best error measures are pointed out at the symw extension technique with an *NRMSE* of 1.04 (6 MAF) and 0.99 (12 MAF) and E_f of −0.08 (6 MAF) and 0 (12 MAF). It is seen that the prediction performances are weaker compared to those of the previous site results. Particularly, E_f values, being close to zero in both cases, could lead to a situation that the predictions might be fluctuating around the mean of the time series. After examining the results of sites 3 and 4, it is observed that the predictions of 6 MAF are better than that of 12 MAF. In case of site 3, under 12 MAF, an optimum *NRMSE* of 1.07 and corresponding E_f value of −0.18 are obtained. This could result in smoother predictions with a lesser possibility of obtaining peak values. Similar interpretation can be drawn from the results of site 4 forecasts. In case of rainfall predictions, both sites 5 and 6 performed better in case of 6 MAF with low *NRMSE* values of 0.65 (site 5) and 0.62 (site 6). Correspondingly E_f values also indicated good predictions in these cases. Under the scenario of 12 MAF, performance measures suggested that sites 5 and 6 could result in smoother predictions of the time series.

When the results are examined from the standpoint of extension technique to be utilized for forecasting, it is seen that the optimum predictions are obtained at different extensions without any consistency, for both 6 MAF and 12 MAF. Also, at rainfall sites, significant differences in the values of *NRMSE* (Table 6) are observed across extensions methods particularly in the case 6 MAF. So, it can be said that one cannot conclude upon the kind of extension method to be used with time series and also choice of extension method shall be an important factor in deciding the final forecasts.

In case of EMD based forecasting, the prediction results obtained across six sites for 6 MAF and 12 MAF through *NRMSE* and E_f measures are presented in Table 8. It is observed that in general, EMD based forecasting algorithm underperformed when compared with results from wavelet based forecasting methodology under both the scenarios of 6 MAF and 12 MAF. Also, even in this method, rainfall predictions in Table 8 are observed to be better than streamflow forecasts. From the results of *NRMSE* it is seen that in almost all the sites, 12 MAF yielded better results than 6 MAF. From the results of E_f, it is inferred that EMD method would have failed in predicting the peaks of the validation time series across all the selected sites of the study. The forecasts selected from Tables 6 and 8 are presented site wise as well as prediction scenario wise (6 MAF and 12 MAF) with each plot containing predictions pertaining to two methods. Figs. 9–12 represent respectively the 6 MAF and 12 MAF results obtained from wavelet based method and EMD based method across all the sites.

It is observed from Figs. 9 and 11 that, wavelet based analyses, in most of the sites, have shown capabilities in predicting higher extremes to an extent considering large time steps ahead of which forecasts are made. This could turn out to be a critical factor in the case of streamflow and rainfall and most importantly for a forecast of longer time steps since there is a possibility of smoothening which does not give much information.

Table 6
NRMSE values for 6, 12 months ahead prediction across sites for wavelet based time series analysis by five extension methods.

Site	Wavelet based method									
	6 months ahead forecast error					12 months ahead forecast error				
	sym	symw	asym	asymw	sp0	sym	symw	asym	asymw	sp0
1	0.84	0.96	1.17	0.94	*0.81*	0.85	0.92	1.00	***0.82***	***0.82***
2	1.10	***1.04***	1.19	1.13	1.08	1.22	***0.99***	1.17	1.38	1.19
3	1.01	1.02	1.17	0.99	***0.98***	1.15	1.08	1.15	1.23	***1.07***
4	1.19	1.11	1.27	***0.99***	1.31	***1.04***	1.10	1.33	1.52	1.35
5	***0.65***	0.82	1.03	0.76	0.66	0.96	***0.95***	1.08	0.99	0.98
6	0.70	0.90	1.04	***0.62***	0.73	0.99	0.93	0.94	***0.91***	0.97

Table 7
E_f values for 6, 12 months ahead prediction across sites for wavelet based time series analysis by five extension methods.

Site	Wavelet based method									
	6 months ahead forecast error					12 months ahead forecast error				
	sym	symw	asym	asymw	sp0	sym	symw	asym	asymw	sp0
1	0.29	0.07	−0.38	0.12	0.35	0.27	0.15	0.00	0.32	0.32
2	−0.21	−0.08	−0.43	−0.29	−0.18	−0.51	0.00	−0.38	−0.92	−0.43
3	−0.03	−0.07	−0.40	0.00	0.02	−0.36	−0.18	−0.34	−0.54	−0.18
4	−0.44	−0.26	−0.64	0.00	−0.75	−0.09	−0.24	−0.81	−1.35	−0.87
5	0.58	0.31	−0.07	0.42	0.55	0.08	0.08	−0.18	0.01	0.03
6	0.50	0.19	−0.09	0.61	0.46	0.01	0.12	0.10	0.16	0.06

Table 8
NRMSE and E_f results for 6, 12 months ahead prediction across sites for EMD based time series analysis.

Performance measure	Forecast	Site					
		1	2	3	4	5	6
EMD based method							
NRMSE	6 Months ahead	1.01	1.17	1.11	1.39	0.94	0.97
	12 Months ahead	0.92	1.04	1.05	1.11	1.02	0.96
E_f	6 Months ahead	−0.03	−0.37	−0.26	−0.97	0.10	0.05
	12 Months ahead	0.14	−0.09	−0.12	−0.24	−0.06	0.07

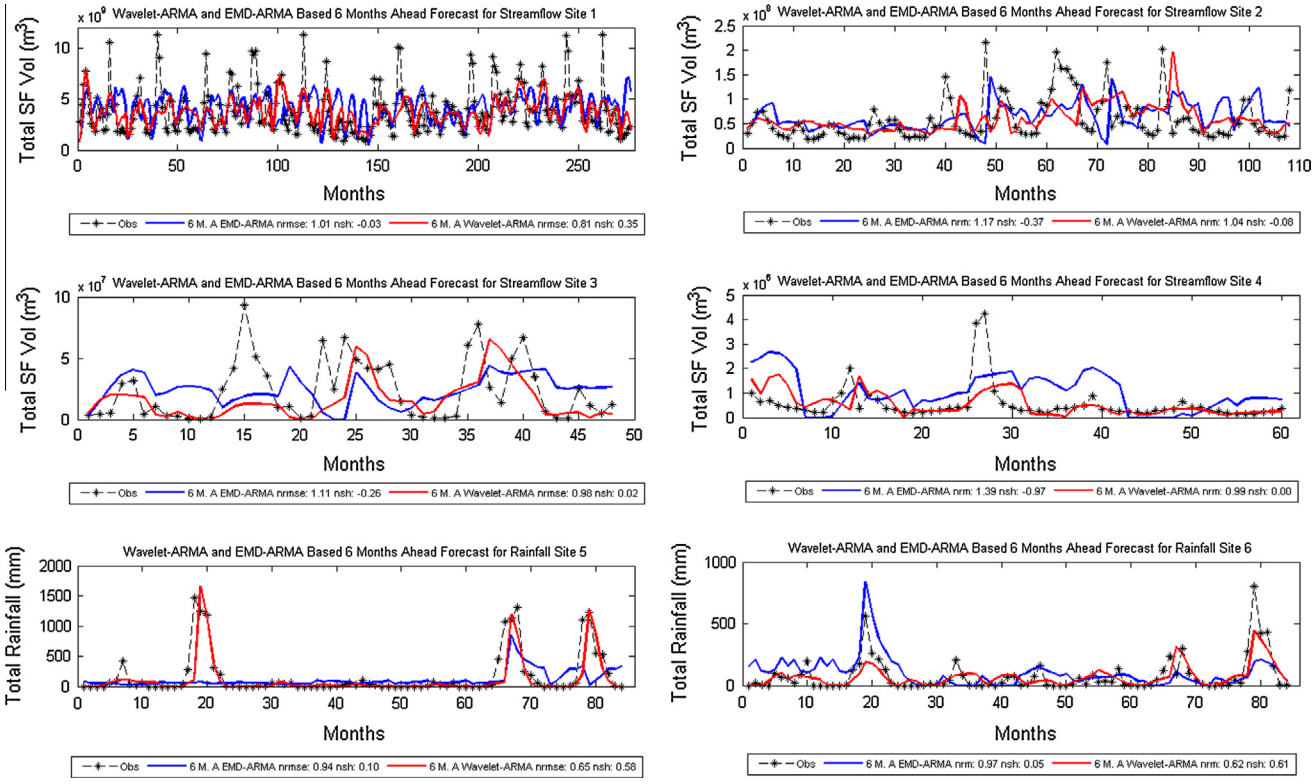

Fig. 9. Prediction plots of six months ahead forecasts for six sites obtained based on wavelet based and EMD based time series analysis.

Also, it can be inferred from scatter plots (Figs. 10 and 12) that the methods managed to capture the minima of the time series effectively under both the scenarios of 6 MAF and 12 MAF. This aspect can be utilized in identifying dry periods in future with a reasonable accuracy which can be attributed to possibility of future droughts.

In the case of 6 MAF in Fig. 9, wavelet based method performed well in estimating the peaks, although it failed to identify multi peaks around same time scale. It is observed from the plots that in most of the sites, 12 MAF (Fig. 11) are smoothened versions of data fluctuating around mean for wavelet based predictions.

Furthermore, EMD based method, in general failed to predict efficiently in both the scenarios (6, 12 MAF) as specified by the previously presented corresponding performance measures. Figs. 10 and 12 point out that the EMD based forecasts (represented by blue dots) are slightly tending towards the mean of the data.

Impact of record lengths in case of streamflows (sites 1 and 2 of Figs. 9 and 11) did not have any effect in forecast results for both the methodologies. This could be due to the reason that the model updation is carried out as blocks of data during calibration and validation phases of the two methods (step 10 of Sections 5 and 6) due to which the forecasting quality depends solely on block length and is independent of data length.

Among the sites with high coefficient of variation (sites 3 and 4 of Figs. 9 and 11), site 3 has performed well with both methods in tending to predict peaks for 6 MAF case although 12 MAF is smoothened around the mean value. In case of site 4, the predictions were poor. This could be because, it can be observed that most of the values are skewed towards the low discharge values and very few peaks are observed which increased the range of observed values. Effectively, although coefficients of variation remained high, values have occurred in the lower end of streamflows which might make even the component time series behave in similar fashion. Due to this, there can be a possibility that time series models can model only lower values giving lesser weight to peaks leading to poorer final predictions than that of site 3.

It is observed from the plots of site 3 in Figs. 9 and 11 that the peaks have not been predicted properly in either of the methods. In case of wavelet based method, this could be because the peaks are considered under low frequency events which are filtered accordingly by approximation or to some extent, by higher level details depending up on the number of levels to which decomposition is made. When these components in particular are not modeled properly, this could be resulting in poorer prediction of peaks. So, an improved methodology would be to model these components

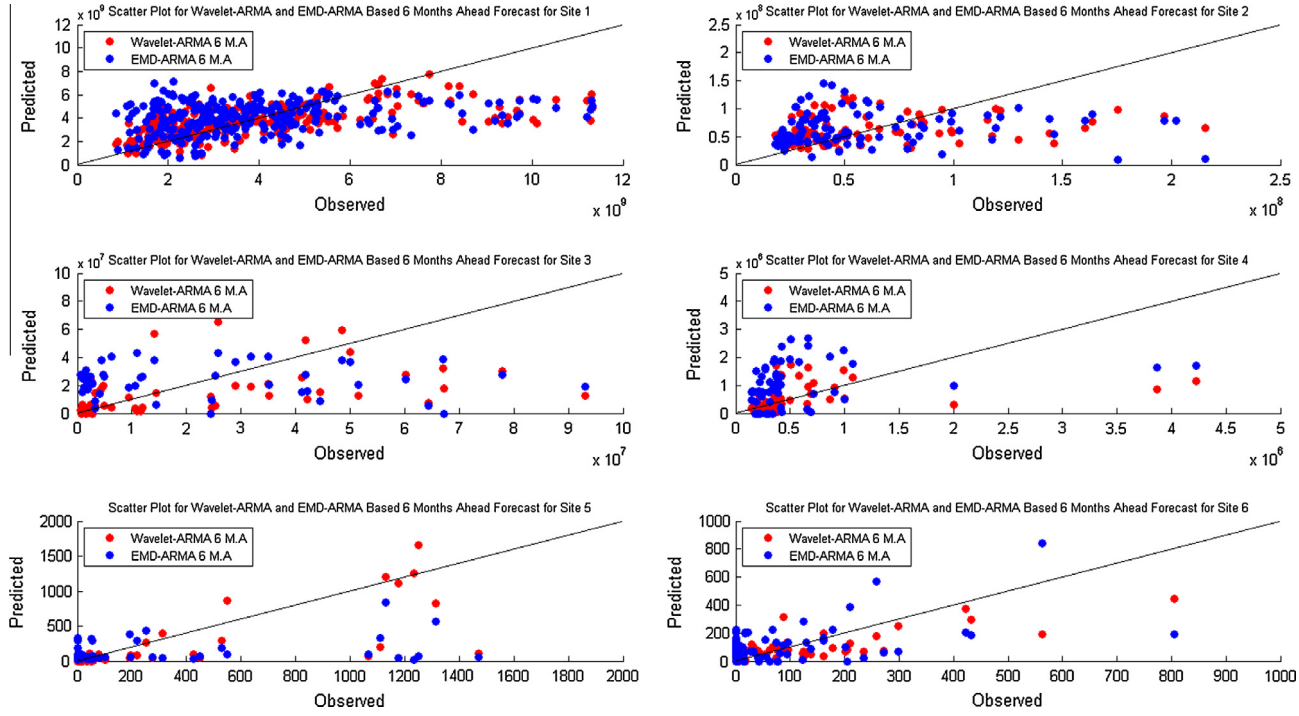

Fig. 10. Scatter plots of six months ahead forecasts for six sites obtained based on wavelet based and EMD based time series analysis.

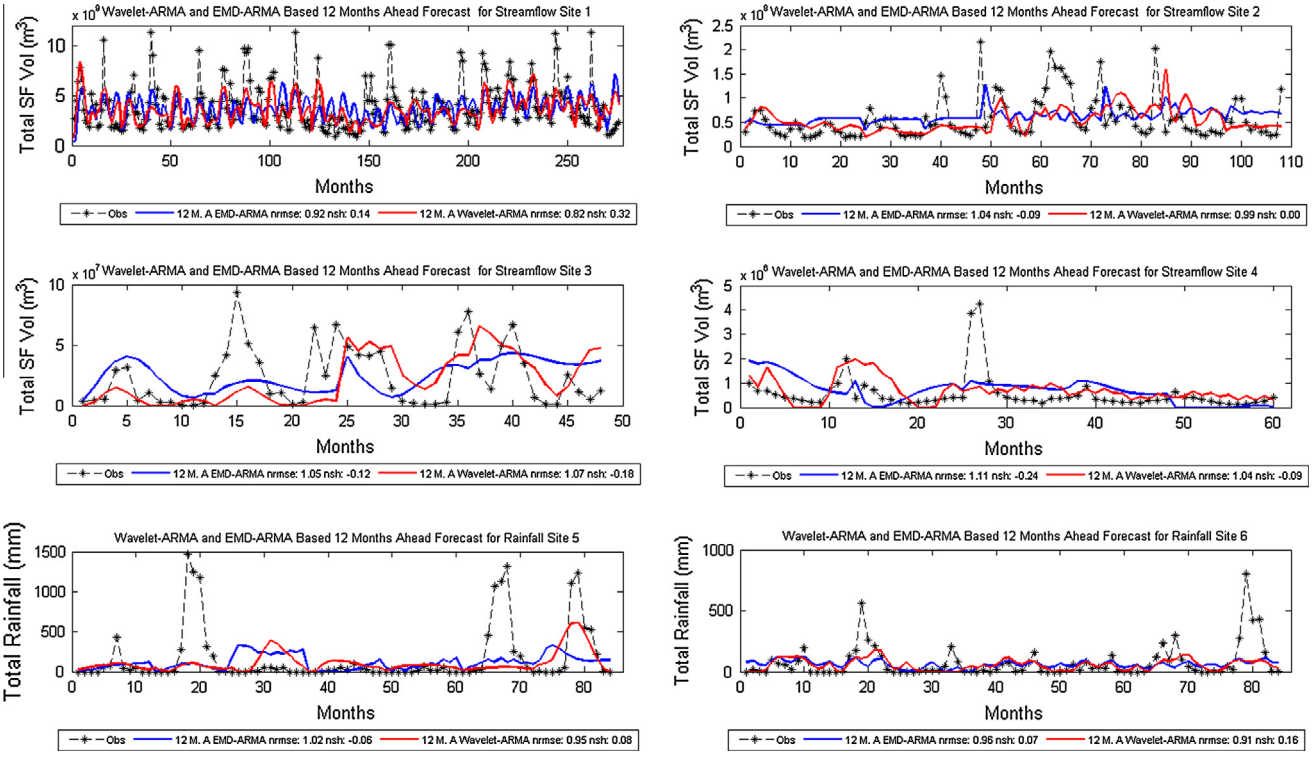

Fig. 11. Prediction plots of twelve months ahead forecasts for six sites obtained based on wavelet based and EMD based time series analysis.

separately by some advanced forecasting technique, obtain the forecasts, model rest of the components using standard time series techniques, obtain the forecasts, add the forecasts of all the components and check the predictability of the models. Similar explanation could be applied in the case of EMD based technique. In this case, low frequency capturing IMFs can be modeled separately using advanced forecasting methods with rest of the IMFs being forecasted by presently applied ARMA models and finally combine the predicted components to obtain time series forecast.

Supporting the performance measures that are obtained previously, prediction plots of rainfall sites 5 and 6 in Fig. 9 demonstrate that the wavelet based method yielded better 6 MAF compared to

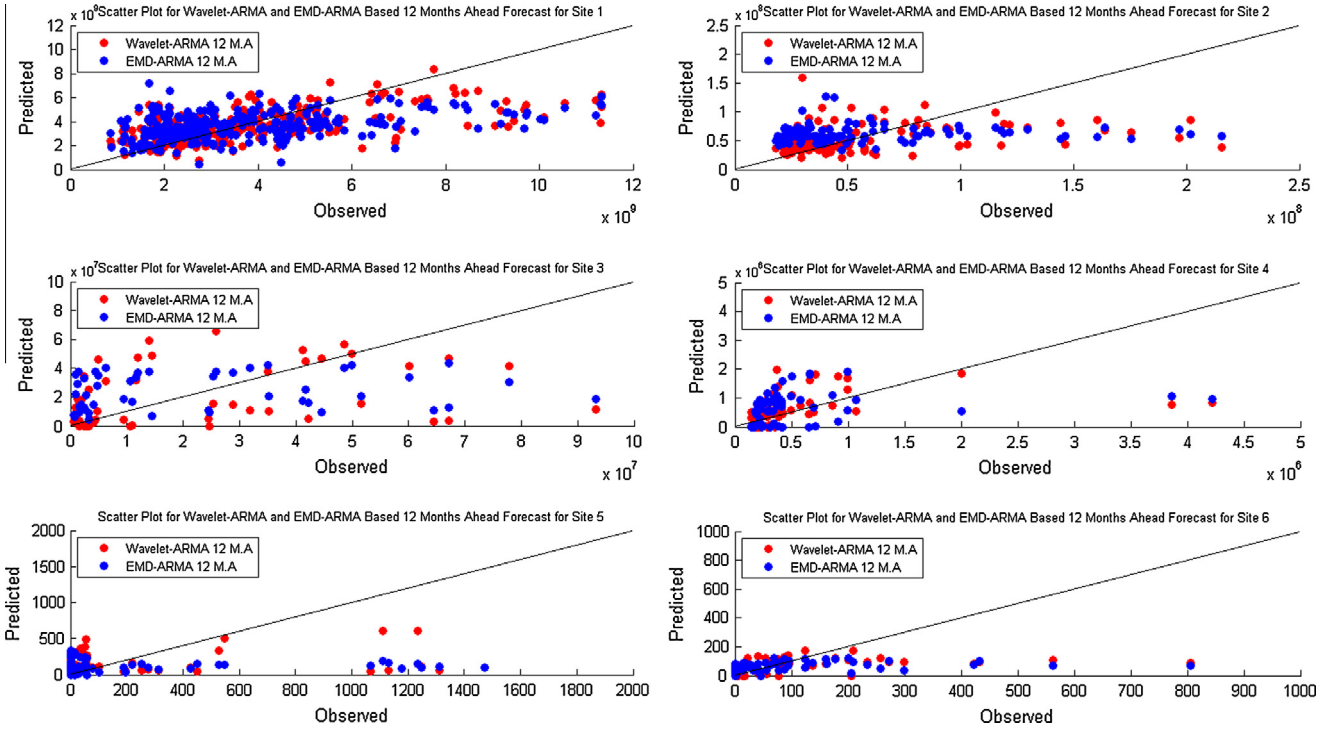

Fig. 12. Scatter plots of twelve months ahead forecasts for six sites obtained based on wavelet based and EMD based time series analysis.

EMD based method. So, it can be said that, with the current setup, wavelet based algorithm can be applied for obtaining accurate rainfall predictions at 6 MAF scenario.

Along with the present wavelet algorithm, decomposition methodology followed by Zhou et al. (2008) is applied over site 1 data without using predictor–corrector model (that was used in the later part of their work) at the end. The algorithm of Zhou et al. (2008) involves decomposing entire data into components and later calibrating and validating each component separately. This does not agree with present method. It is observed that forecasts through the method of Zhou et al. (2008) were very accurate when compared with present results. Fig. 13 shows the prediction plot of 6 MAF and 12 MAF.

But, since the data is being decomposed first and later the components are being divided into calibration and validation datasets, some amount of future (validation) information is being sent into the calibration system which is a modeling mistake. The proper way of modeling would be to use data, decompose, forecast certain number of values in components, at the end of which observed values are recorded, append these to previously used data, perform decomposition again, forecast next set of values and so on. So, during this process, data is being sent as blocks due to which there are several breakages at the ends. These breakages in data lead to boundary distortions when wavelet decomposition algorithm is applied. In order to explain this, an experiment is carried out where data decompositions were made in two cases, one in which initially a 150 length data is subjected to one level decomposition algorithm using db5 mother wavelet to obtain an approximation and detail. In the second case, data is broken down into three sub datasets each of 50 length and each of these sets are subjected

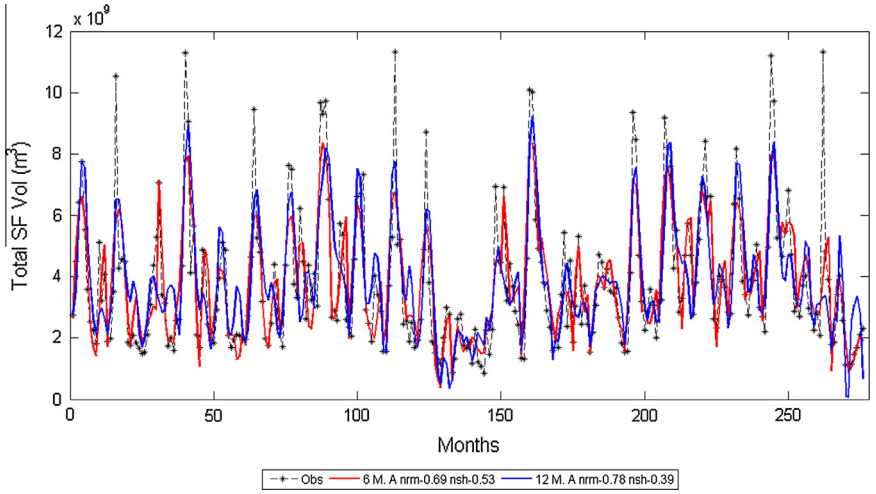

Fig. 13. Wavelet based six months and twelve months ahead forecasts for site 1 obtained through the methodology of Zhou et al. (2008).

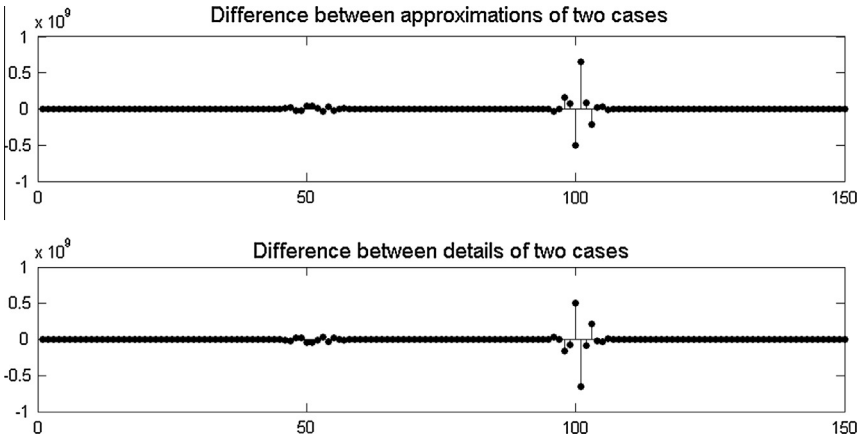

Fig. 14. Stem plots of differences between respective approximations and details of two cases.

individually to one level wavelet decomposition algorithm using same db5 mother wavelet. Later the three approximations and three detail sets obtained from case two are appended respectively to obtain final approximation and detail sequences each of 150 length that can be matched with the results of the first case. In both the situations, symmetric extension method is used. Fig. 14 shows plots of difference between respective approximations and details of the two cases.

From Fig. 14, it is observed that, in both approximation and detail, at the joints i.e., at 50 and 100, significant spikes are observed whereas for rest of the length the difference is zero. The occurrence of spikes is due to the effect of boundary distortion. The rest of the extension methods, though tried to reduce the variation, were not successful enough in bringing the absolute difference to zero at boundaries. Similar effects are observed in case of EMD with its IMFs and residual at boundaries. This effect of boundary distortion could be minimal in case of application of wavelets and EMD in compression or denoising. For the present study, values at the joints are of paramount importance since these are the values that are modeled by ARMA.

Integrating the inferences from results and experiment conducted, it can be said that effects of the models are twofold. One, at the stage of decomposition, wavelets and EMD have significant boundary distortions in their components. The values at boundaries are critical for component time series modeling. Two, modeling and forecasting the component time series for larger time steps ahead such as 6 and 12 months might make the predictions smoother not being able to capture the extremes of the data. On the other hand, with these algorithms, prediction of shorter time steps such as 1 month ahead does not make sense as the models turn out to be computationally very expensive. So, there has to be a clear tradeoff between boundary effects and component modeling in influencing the results. It is interpreted that an inverse relation exists between the number of times decomposition algorithm need to be employed and the number of time steps ahead of which forecasts are needed to be obtained. Suppose, if one does require to forecast both 6 MAF and 12 MAF of ten years of monthly time series using the proposed decomposition based forecasting algorithms, it so happens that in the case of 6 MAF, due to lesser number of time steps, time series methods would yield better predictions but on the other hand, the decomposition algorithms need to be employed 20 times due to which the error that occurs due to time series distortion at the ends also increases simultaneously. At the same time, in the case of 12 MAF, time series algorithms are needed to be used only 10 times which would decrease the error due to distortions but simultaneously, smoother predictions are expected from time series models due to greater time steps ahead increasing the forecast error.

Now, it is seen from Table 8 that the predictions of 12 MAF are better than that of 6 MAF in the case of EMD based forecasting results. From the inverse relation explained above, it can be interpreted that the better performance of 12 MAF could be due to stronger impact of boundary distortions occurring during application of EMD over the effect of smoothening due to longer time steps ahead predictions. This situation did not occur with the wavelet based method's predictions which could be due to stronger impact of weaker prediction capabilities of time series models (inability to yield accurate predictions at lager time steps ahead such as 12 MAF) over the effect of border distortions due to wavelet decomposition.

So, to deal with boundary effects, some more extension methods can be explored both in wavelets as well as EMD. In case of wavelets, the algorithm can be applied to some other wavelet function (such as symlets and biorthogonal wavelets) that have effects on the components accordingly. When it comes to component modeling, model selection criteria can be altered to verify if better models are selected. Research can be carried out in extending the domain of time series models that are applied to components of such nonlinear time series models which can model the components efficiently despite boundary effects.

8. Conclusions

For the present work, the predictability of wavelet based and EMD based time series modeling techniques are studied under various case studies of monthly total streamflow (four non-stationary sites) and monthly total rainfall (two non-stationary sites) locations. The basic modeling technique in both algorithms is to decompose a time series into components and forecast them individually, the reconstruction of which yields future time series predictions. The results indicate that both the models have predicted the lower extremes of time series at longer time steps ahead from which it can be said that the algorithms can be used to model droughts despite stationarity issues which is an important factor for tropical countries like India.

With the current setup, wavelet based algorithm can be applied to rainfall data to result in accurate 6 months ahead forecasts.

Further research can be undertaken to modify extension techniques in both the models in order to suppress the boundary effects or a possibility of using different wavelet all together can also be explored. The domain of modeling techniques applied to components can be shifted towards nonlinear time series models that can read the boundary effects more efficiently.

With a reasonable accuracy, wavelets based method is preferable over EMD based method in predicting some of the maxima in

the data at lesser time steps ahead such as six months. So, modifying the model parameters of wavelet algorithm such as mother wavelet, model selection criteria and pitching in nonlinear time series analysis, there is a rich possibility that the wavelet algorithms can be even used to for flood modeling.

References

Adamowski, J., Chan, H.F., 2011. A wavelet neural network conjunction model for groundwater level forecasting. J. Hydrol. 407 (1), 28–40.

Adamowski, K., Prokoph, A., Adamowski, J., 2009. Development of a new method of wavelet aided trend detection and estimation. Hydrol. Process. 23 (18), 2686–2696.

Akaike, H., 1974. A new look at the statistical model identification. IEEE Trans. Autom. Control 19 (6), 716–723.

Akaike, H., 1978. A Bayesian analysis of the minimum AIC procedure. Ann. Inst. Stat. Math. 30 (1), 9–14.

Almasri, A., Locking, H., Shukur, G., 2008. Testing for climate warming in Sweden during 1850–1999, using wavelets analysis. J. Appl. Stat. 35 (4), 431–443.

Anderson, O., 1927. On the logic of the decomposition of statistical series into separate components. J. Roy. Stat. Soc. 90 (3), 548–569.

Armstrong, J.S., 1989. Combining forecasts: the end of the beginning or the beginning of the end? Int. J. Forecast. 5 (4), 585–588.

Asefa, T., Kemblowski, M., McKee, M., Khalil, A., 2006. Multi-time scale stream flow predictions: the support vector machines approach. J. Hydrol. 318 (1), 7–16.

Baker, W.L., 1990. Climatic and hydrologic effects on the regeneration of *Populus angustifolia* James along the Animas River, Colorado. J. Biogeogr., 59–73.

Bayazit, M., Aksoy, H., 2001. Using wavelets for data generation. J. Appl. Stat. 28 (2), 157–166.

Boashash, B., 1992. Estimating and interpreting the instantaneous frequency of a signal. I. Fundamentals. Proc. IEEE 80 (4), 520–538.

Box, G.E., Jenkins, G.M., Reinsel, G.C., 1970. Time Series Analysis Forecasting and Control. Holden Day, San Francisco.

Bras, R.L., Rodríguez-Iturbe, I., 1985. Random Functions and Hydrology. Addison-Wesley, Reading, Mass.

Brown, R.G., 1962. Smoothing, Forecasting and Prediction of Discrete Time Series. Prentice Hall, Englewood Cliffs, NJ.

Brown, R.G., Meyer, R.F., 1961. The fundamental theorem of exponential smoothing. Oper. Res. 9 (5), 673–685.

Chambers, J.C., Mullick, S.K., Smith, D.D., 1974. An Executive's Guide to Forecasting. Wiley.

Chambers, J.C., Smith, D.D., Mullick, S.K., 1971. How to Choose the Right Forecasting Technique. Harvard University, Graduate School of Business Administration.

Chang, F.J., Chiang, Y.M., Chang, L.C., 2007. Multi-step-ahead neural networks for flood forecasting. Hydrol. Sci. J. 52 (1), 114–130.

Chen, P.A., Chang, L.C., Chang, F.J., 2013. Reinforced recurrent neural networks for multi-step-ahead flood forecasts. J. Hydrol. 497, 71–79.

Chen, Y.H., Chang, F.J., 2009. Evolutionary artificial neural networks for hydrological systems forecasting. J. Hydrol. 367 (1), 125–137.

Chui, C.K., 1992. An Introduction to Wavelets. Academic Press Professional, Inc..

Cohen, A., Daubechies, I., Vial, P., 1993. Wavelets on the interval and fast wavelet transforms. Appl. Comput. Harmon. Anal. 1 (1), 54–81.

Daubechies, I., 1988. Orthonormal bases of compactly supported wavelets. Commun. Pure Appl. Math. 41 (7), 909–996.

Daubechies, I., 1992. Ten Lectures on Wavelets, vol. 61. Society for industrial and applied mathematics, Philadelphia, PA.

de Queiroz, R.L., 1992. Subband processing of finite length signals without border distortions. IEEE Int. Conf. Acoust. Speech Signal Process. ICASSP-92. 4, 613–616.

Duport, G.B., Girel, J., Chassery, J.M., Patou, G., 1996. The use of multiresolution analysis and wavelets transform for merging SPOT panchromatic and multispectral image data. Photogramm. Eng. Remote Sens. 62 (9), 1057–1066.

Elshorbagy, A., Simonovic, S.P., Panu, U.S., 2002. Estimation of missing streamflow data using principles of chaos theory. J. Hydrol. 255 (1), 123–133.

Franchini, M., Bernini, A., Barbetta, S., Moramarco, T., 2011. Forecasting discharges at the downstream end of a river reach through two simple Muskingum based procedures. J. Hydrol. 399 (3), 335–352.

Frisch, R., 1931. A method of decomposing an empirical series into its cyclical and progressive components. J. Am. Stat. Assoc. 26 (173A), 73–78.

Galford, G.L., Mustard, J.F., Melillo, J., Gendrin, A., Cerri, C.C., Cerri, C.E., 2008. Wavelet analysis of MODIS time series to detect expansion and intensification of row-crop agriculture in Brazil. Remote Sens. Environ. 112 (2), 576–587.

Grossmann, A., Morlet, J., 1984. Decomposition of Hardy functions into square integrable wavelets of constant shape. SIAM J. Math. Anal. 15 (4), 723–736.

Gulhane, P., Menezes, B., Reddy, T., Shah, K., Soman, S.A., 2005. Forecasting using decomposition and combinations of experts. Networks (ANNs) 1 (7), 21.

Haar, A., 1910. Zur theorie der orthogonalen funktionensysteme. Math. Ann. 69 (3), 331–371.

Han, P., Wang, P., Tian, M., Zhang, S., Liu, J., Zhu, D., 2013. Application of the ARIMA Models in Drought Forecasting Using the Standardized Precipitation Index. Computer and Computing Technologies in Agriculture VI, pp. 352–358.

Hannan, E.J., Quinn, B.G., 1979. The determination of the order of an autoregression. J. Roy. Stat. Soc. Ser. B – Method., 190–195.

Heil, C.E., Walnut, D.F., 1989. Continuous and discrete wavelet transforms. SIAM Rev. 31 (4), 628–666.

Heisenberg, W., 1925. Quantum-theoretical re-interpretation of kinematic and mechanical relations. Z. Phys. 33, 879–893.

Hibon, M., Evgeniou, T., 2005. To combine or not to combine: selecting among forecasts and their combinations. Int. J. Forecast. 21 (1), 15–24.

Hipel, K.W., McLeod, A.I., Lennox, W.C., 1977. Advances in Box–Jenkins modeling: 1. Model construction. Water Resour. Res. 13 (3), 567–575.

Holt, C.C., 1957. Forecasting Trends and Seasonals by Exponentially Weighted Moving Averages, O.N.R Memorandum 52, Carnegie Institute of Technology, Pittsburg, PA.

Hosking, J.R., 1984. Modelling persistence in hydrological time series using fractional differencing. Water Resour. Res. 20 (12), 1898–1908.

Hou, H., Andrews, H., 1978. Cubic splines for image interpolation and digital filtering. IEEE Trans. Acoust. Speech Signal Process. 26 (6), 508–517.

Huang, N.E., Shen, Z., Long, S.R., Wu, M.C., Shih, H.H., Zheng, Q., Liu, H.H., 1998. The empirical mode decomposition and the Hilbert spectrum for nonlinear and non-stationary time series analysis. Proc. Roy. Soc. Lond. Ser. A: Math. Phys. Eng. Sci. 454 (1971), 903–995.

Huang, N.E., Wu, Z., 2008. A review on Hilbert-Huang transform: method and its applications to geophysical studies. Rev. Geophys. 46 (2).

Kashyap, R.L., Rao, A.R., 1976. Dynamic Stochastic Models from Empirical Data, vol. 122. Academic Press, New York.

Keskin, M.E., Taylan, D., Terzi, O., 2006. Adaptive neural-based fuzzy inference system (ANFIS) approach for modelling hydrological time series. Hydrol. Sci. J. 51 (4), 588–598.

Kişi, Ö., Cimen, M., 2011. A wavelet-support vector machine conjunction model for monthly streamflow forecasting. J. Hydrol. 399 (1), 132–140.

Kişi, Ö., Shiri, J., 2011. Precipitation forecasting using wavelet-genetic programming and wavelet-neuro-fuzzy conjunction models. Water Resour. Manage. 25 (13), 3135–3152.

Kumar, P., Foufoula-Georgiou, E., 1993. A multicomponent decomposition of spatial rainfall fields. 1. Segregation of large- and small-scale features using wavelet transforms. Water Resour. Res. 29 (8), 2515–2532.

Kwiatkowski, D., Phillips, P.C., Schmidt, P., Shin, Y., 1992. Testing the null hypothesis of stationarity against the alternative of a unit root: how sure are we that economic time series have a unit root? J. Econom. 54 (1), 159–178.

Labat, D., 2005. Recent advances in wavelet analyses: Part 1. A review of concepts. J. Hydrol. 314 (1), 275–288.

Lee, T., Ouarda, T.B.M.J., 2012. Stochastic simulation of nonstationary oscillation hydroclimatic processes using empirical mode decomposition. Water Resour. Res. 48 (2).

Lin, J.Y., Cheng, C.T., Chau, K.W., 2006. Using support vector machines for long-term discharge prediction. Hydrol. Sci. J. 51 (4), 599–612.

Loucks, D.P., Stedinger, J.R., Haith, D.A., 1981. Water Resource Systems Planning and Analysis. Prentice-Hall.

Macaulay, F.R., 1931. Introduction to "The Smoothing of Time Series". The Smoothing of Time Series. NBER, pp. 17–30.

Magrin-Chagnolleau, I., Baraniuk, R.G., 1999. Empirical mode decomposition based frequency attributes. In: Proc. SEG Meeting. Houston, Texas, USA.

Makridakis, S., Hibon, M., 1979. Accuracy of forecasting: an empirical investigation (with discussion). J. Roy. Stat. Soc. A 142, 97–145.

Mallat, S., 1987. A compact multiresolution representation: the wavelet model. In: Proc. IEEE Workshop Computer Civion, Miami, FL.

Mallat, S.G., 1989a. A theory for multiresolution signal decomposition: the wavelet representation. IEEE Trans. Pattern Anal. Mach. Intel. 11 (7), 674–693.

Mallat, S.G., 1989b. Multifrequency channel decompositions of images and wavelet models. IEEE Trans. Acoust. Speech Signal Process. 37 (12), 2091–2110.

Mallat, S.G., 1989c. Multiresolution approximations and wavelet orthonormal bases of L2 (R). Trans. Am. Math. Soc. 315(1).

Martínez, B., Gilabert, M.A., 2009. Vegetation dynamics from NDVI time series analysis using the wavelet transform. Remote Sens. Environ. 113 (9), 1823–1842.

McLeod, A.I., Hipel, K.W., Lennox, W.C., 1977. Advances in Box-Jenkins modeling: 2. Applications. Water Resour. Res. 13 (3), 577–586.

McMahon, T.A., Kiem, A.S., Peel, M.C., Jordan, P.W., Pegram, G.G., 2008. A new approach to stochastically generating six-monthly rainfall sequences based on empirical mode decomposition. J. Hydrometeorol. 9 (6), 1377–1389.

Meyer, Y., 1985. Principle d'incertitude, bases Hilbertiennes et algebres d'operateurs. Seminare Bourbaki, pp. 662.

Milly, P.C.D., Julio, B., Malin, F., Robert, M.H., Zbigniew, W.K., Dennis, P.L., Ronald, J.S., 2007. Stationarity is dead. Ground Water News Views 4 (1), 6–8.

Misiti, M., Misiti, Y., Oppenheim, G., Poggi, J., 1996. Wavelet Toolbox Manual—User's Guide. The Math Works Inc., Natick, MA.

Mohammadi, K., Eslami, H.R., Kahawita, R., 2006. Parameter estimation of an ARMA model for river flow forecasting using goal programming. J. Hydrol. 331 (1), 293–299.

Morlet, J., Arens, G., Fourgeau, E., Giard, D., 1982. Wave propagation and sampling theory, Part II. Geophysics 47, 222–236.

Muth, J.F., 1960. Optimal properties of exponentially weighted forecasts. J. Am. Stat. Assoc. 55 (290), 299–306.

Napolitano, G., Serinaldi, F., See, L., 2011. Impact of EMD decomposition and random initialisation of weights in ANN hindcasting of daily stream flow series: an empirical examination. J. Hydrol. 406 (3), 199–214.

Nawab, S.H., Quatieri, T.F., 1988. Short-time Fourier transform. Adv. Top. Signal Process., 289–337.

Nourani, V., Komasi, M., Mano, A., 2009. A multivariate ANN-wavelet approach for rainfall–runoff modelling. Water Resour. Manage 23 (14), 2877–2894.
Papademetriou, M., Tachtsidis, I., Elliott, M.J., Hoskote, A., Elwell, C.E., 2013. Wavelet cross-correlation to investigate regional variations in cerebral oxygenation in infants supported on extracorporeal membrane oxygenation. Oxygen Transport to Tissue 34, 203–209.
Partal, T., Kişi, Ö., 2007. Wavelet and neuro-fuzzy conjunction model for precipitation forecasting. J. Hydrol. 342 (1), 199–212.
Pegels, C.C., 1969. Exponential forecasting: some new variations. Manage. Sci. 12, 311–315.
Pegram, G.G.S., Salas, J.D., Boes, D.C., Yevjevich, V.M., 1980. Stochastic Properties of Water Storage. Colo. State Univ, Fort Collins.
Preis, A., Ostfeld, A., 2008. A coupled model tree–genetic algorithm scheme for flow and water quality predictions in watersheds. J. Hydrol. 349 (3), 364–375.
Rajeevan, M., Bhate, J., 2009. A high resolution daily gridded rainfall data set (1971–2005) for mesoscale meteorological studies. Curr. Sci. 96 (4), 558–562.
Rao, R.M., Bopardikar, A.S., 1998. Wavelet Transforms: Introduction to Theory and Applications, vol. 20. Addison–Wesley Longman, Inc., pp. 604–618
Rilling, G., Flandrin, P., Gonçalvés, P., 2003. On empirical mode decomposition and its algorithms. IEEE-EURASIP Workshop on Nonlinear Signal and Image Processing NSIP, vol. 3, pp. 8–11.
Rissanen, J., 1978. Modelling by shortest data description. Automatica 14 (5), 465–471.
Salas, J.D., Delleur, J.W., Yevjevich, V.M., Lane, W.L., 1980. Applied Modeling of Hydrologic Time Series. Water Resources Publications, Littleton, Colo.
Sang, Y.F., 2012. A review on the applications of wavelet transform in hydrology time series analysis. Atmos. Res. 122, 8–15.
Sang, Y.F., Wang, D., Wu, J.C., 2010. Entropy-based method of choosing the decomposition level in wavelet threshold de-noising. Entropy 12 (6), 1499–1513.
Sang, Y.F., Wang, Z., Liu, C., 2012a. Discrete wavelet-based trend identification in hydrologic time series. Hydrol. Process.. http://dx.doi.org/10.1002/hyp.9356.
Sang, Y.F., Wang, Z., Liu, C., 2012b. Period identification in hydrologic time series using empirical mode decomposition and maximum entropy spectral analysis. J. Hydrol. 424, 154–164.
Schwarz, G., 1978. Estimating the dimension of a model. Ann. Stat. 6 (2), 461–464.
Seghouane, A.K., Bekara, M., 2004. A small sample model selection criterion based on Kullback's symmetric divergence. IEEE Trans. Signal Process. 52 (12), 3314–3323.
Shibata, R., 1980. Asymptotically efficient selection of the order of the model for estimating parameters of a linear process. Ann. Stat. 147–164.
Simonovic, S.P., 1995. Synthesizing missing streamflow records on several Manitoba streams using multiple nonlinear standardized correlation analysis. Hydrol. Sci. J. 40 (2), 183–203.
Slack, J.R., Landwehr, J.M., 1994. Hydro-Climatic Data Network (HCDN) Streamflow Data Set: US Geological Survey Water-Resources Investigations Report. CD-ROM Disk, 93-4076.
Starrett, S.K., Heier, T., Su, Y., Tuan, D., Bandurraga, M., 2010. Filling in missing peak flow data using artificial neural networks. ARPN J. Eng. Appl. Sci. 5 (1).
Stedinger, J.R., Lettenmaier, D.P., Vogel, R.M., 1985. Multisite ARMA (1,1) and disaggregation models for annual streamflow generation. Water Resour. Res. 21 (4), 497–509.
Stedinger, J.R., Vogel, R.M., 1984. Disaggregation procedures for generating serially correlated flow vectors. Water Resour. Res. 20 (1), 47–56.
Strang, G., Nguyen, T., 1996. Wavelets and Filter Banks. Cambridge University Press.
Tan, Z., Lu, B., Sun, Y., Sun, Y., Huang, S., 2011. Wavelet analysis of $\delta^{18}O$ time series of monthly precipitation. Int. Conf. Remote Sens. Environ. Transport. Eng. (RSETE), 8731–8734.
Tay, D.B., Kingsbury, N.G., 1993. Flexible design of multidimensional perfect reconstruction FIR 2-band filters using transformations of variables. IEEE Trans. Image Process. 2 (4), 466–480.
Temraz, H.K., Salama, M.M.A., Quintana, V.H., 1996. Application of the decomposition technique for forecasting the load of a large electric power network. IEE Proc. Gener. Transm. Distrib. 143 (1), 13–18.
Toth, E., Brath, A., Montanari, A., 2000. Comparison of short-term rainfall prediction models for real-time flood forecasting. J. Hydrol. 239 (1), 132–147.
Vishwanath, M., 1994. The recursive pyramid algorithm for the discrete wavelet transform. IEEE Trans. Signal Process. 42 (3), 673–676.
Voss, M.S., Feng, X., 2002. ARMA model selection using particle swarm optimization and AIC criteria. In: Proc. 15th IFAC World Congress on Automatic Control.
Wang, L., Gupta, S., 2013. Neural networks and wavelet de-noising for stock trading and prediction. Time Ser. Anal. Modell. Appl. ISRL 47, 229–247.
Wang, W., Ding, J., 2003. Wavelet network model and its application to the prediction of hydrology. Nat. Sci. 1 (1), 67–71.
Wei, S., Yang, H., Song, J., Abbaspour, K., Xu, Z., 2013. A wavelet-neural network hybrid modelling approach for estimating and predicting river monthly flows. Hydrol. Sci. J., 1–16.
Weng, H., Lau, K.M., 1994. Wavelets, period doubling, and time–frequency localization with application to organization of convection over the tropical western Pacific. J. Atmos. Sci. 51, 2523–2541.
Wiener, N., 1949. The Extrapolation, Interpolation and Smoothing of Stationary Time Series with Engineering Applications. Wiley, New York.
Winters, P.R., 1960. Forecasting sales by exponentially weighted moving averages. Manage. Sci. 6 (3), 324–342.
Worrall, F., Swank, W.T., Burt, T.P., 2003. Changes in stream nitrate concentrations due to land management practices, ecological succession, and climate: developing a systems approach to integrated catchment response. Water Resour. Res. 39 (7), 1177.
Xiao-jie, X., Si-xia, H., Qiang, H., Yan, L., 2008. The application of wavelet analysis in hydrological sequence trend analysis. In: The 2nd Int. Conf. Bioinformatics and Biomedical Engineering. ICBBE, pp. 3495–3498.
Yevjevich, V.M., 1972. Stochastic Processes in Hydrology. Water Resources Publications, Fort Collins, Colorado.
Yu, G.B., Huang, L., Dai, B., Wu, X.M., Ma, W.S., 2013. Reducer vibration de-noising signal research based on wavelet transform. Appl. Mech. Mater. 274, 225–228.
Zheng, J., Peng, S.P., Liu, M.C., Liang, Z., 2013. A novel seismic wavelet estimation method. J. Appl. Geophys. 90, 92–95.
Zhou, H.C., Peng, Y., Liang, G.H., 2008. The research of monthly discharge predictor–corrector model based on wavelet decomposition. Water Resour. Manage. 22 (2), 217–227.
Zou, H., Yang, Y., 2004. Combining time series models for forecasting. Int. J. Forecast. 20 (1), 69–84.